AFRL-OSR-VA-TR-2015-0105

NEW SYNTHETIC AND ASSEMBLY METHODOLOGY FOR GUIDING NANOMATERIAL ASSEMBLY WITH HI

Mathew Maye
SYRACUSE UNIVERSITY

04/06/2015
Final Report

Air Force Research Laboratory
AF Office Of Scientific Research (AFOSR)/ RTD
Arlington, Virginia 22203
Air Force Materiel Command

REPORT DOCUMENTATION PAGE

Form Approved
OMB No. 0704-0188

PLEASE DO NOT RETURN YOUR FORM TO THE ABOVE ORGANIZATION.

1. REPORT DATE *(DD-MM-YYYY)*	2. REPORT TYPE	3. DATES COVERED *(From - To)*
26-03-2015	Final	01/01/2010 - 12/31/2014

4. TITLE AND SUBTITLE
New Synthetic and Assembly Methodology for Guiding Nanomaterial Assembly with High Fidelity into ID cluster and 3D Crystals Using Biomimetic Interactions

5a. CONTRACT NUMBER

5b. GRANT NUMBER
FA9550-10-1-0033

5c. PROGRAM ELEMENT NUMBER

6. AUTHOR(S)
Maye, Mathew

5d. PROJECT NUMBER

5e. TASK NUMBER

5f. WORK UNIT NUMBER

7. PERFORMING ORGANIZATION NAME(S) AND ADDRESS(ES)
Syracuse University
Office of Sponsored Programs
113 Bowne Hall
Syracuse, NY 13244-1200

8. PERFORMING ORGANIZATION REPORT NUMBER
N/A

9. SPONSORING/MONITORING AGENCY NAME(S) AND ADDRESS(ES)
USAF/AFRL
AF Office of Scientific Research
875 No. Randolph St.
Arlington, VA 22203

10. SPONSOR/MONITOR'S ACRONYM(S)
N/A

11. SPONSOR/MONITOR'S REPORT NUMBER(S)
N/A

12. DISTRIBUTION/AVAILABILITY STATEMENT
N/A

13. SUPPLEMENTARY NOTES
N/A

14. ABSTRACT

In year five of our grant we successfully completed a major grant milestone, and made progress and improvements in the areas where goals have previously been met. These accomplishments include: the first publication in the field on the self-assembly of quantum rods using DNA in which we used a patterned surface provided by DNA origami to control rod alignment and spacing (Section 1); published final results showing bioluminescence resonance energy transfer between firefly luciferase enzymes and rods that emit near infrared light (nIR), and improved long term stability and activity of the BRET nanoconjugates (Section 2). Finally, we completed a study that investigated ways to manipulate the 3D assembly of DNA-capped gold nanoparticles by using smart pH sensitive co-polymers, and transitioned that system to using elastin like polypeptides that have similar thermal- and pH responsive behavior (Section 3). We also successfully aquired and set-up an atomic force microscope purchased with AFOSR support. Two high impact articles were published, and one is in review. Four additional papers cite the grant, and three papers are in final stages of preparation.

15. SUBJECT TERMS

16. SECURITY CLASSIFICATION OF:			17. LIMITATION OF ABSTRACT	18. NUMBER OF PAGES	19a. NAME OF RESPONSIBLE PERSON
a. REPORT	b. ABSTRACT	c. THIS PAGE			Mathew Maye
U	U	U	SAR	48	19b. TELEPHONE NUMBER *(Include area code)* 315-443-2146

INSTRUCTIONS FOR COMPLETING SF 298

1. REPORT DATE. Full publication date, including day, month, if available. Must cite at least the year and be Year 2000 compliant, e.g. 30-06-1998; xx-06-1998; xx-xx-1998.

2. REPORT TYPE. State the type of report, such as final, technical, interim, memorandum, master's thesis, progress, quarterly, research, special, group study, etc.

3. DATES COVERED. Indicate the time during which the work was performed and the report was written, e.g., Jun 1997 - Jun 1998; 1-10 Jun 1996; May - Nov 1998; Nov 1998.

4. TITLE. Enter title and subtitle with volume number and part number, if applicable. On classified documents, enter the title classification in parentheses.

5a. CONTRACT NUMBER. Enter all contract numbers as they appear in the report, e.g. F33615-86-C-5169.

5b. GRANT NUMBER. Enter all grant numbers as they appear in the report, e.g. AFOSR-82-1234.

5c. PROGRAM ELEMENT NUMBER. Enter all program element numbers as they appear in the report, e.g. 61101A.

5d. PROJECT NUMBER. Enter all project numbers as they appear in the report, e.g. 1F665702D1257; ILIR.

5e. TASK NUMBER. Enter all task numbers as they appear in the report, e.g. 05; RF0330201; T4112.

5f. WORK UNIT NUMBER. Enter all work unit numbers as they appear in the report, e.g. 001; AFAPL30480105.

6. AUTHOR(S). Enter name(s) of person(s) responsible for writing the report, performing the research, or credited with the content of the report. The form of entry is the last name, first name, middle initial, and additional qualifiers separated by commas, e.g. Smith, Richard, J, Jr.

7. PERFORMING ORGANIZATION NAME(S) AND ADDRESS(ES). Self-explanatory.

8. PERFORMING ORGANIZATION REPORT NUMBER. Enter all unique alphanumeric report numbers assigned by the performing organization, e.g. BRL-1234; AFWL-TR-85-4017-Vol-21-PT-2.

9. SPONSORING/MONITORING AGENCY NAME(S) AND ADDRESS(ES). Enter the name and address of the organization(s) financially responsible for and monitoring the work.

10. SPONSOR/MONITOR'S ACRONYM(S). Enter, if available, e.g. BRL, ARDEC, NADC.

11. SPONSOR/MONITOR'S REPORT NUMBER(S). Enter report number as assigned by the sponsoring/ monitoring agency, if available, e.g. BRL-TR-829; -215.

12. DISTRIBUTION/AVAILABILITY STATEMENT. Use agency-mandated availability statements to indicate the public availability or distribution limitations of the report. If additional limitations/ restrictions or special markings are indicated, follow agency authorization procedures, e.g. RD/FRD, PROPIN, ITAR, etc. Include copyright information.

13. SUPPLEMENTARY NOTES. Enter information not included elsewhere such as: prepared in cooperation with; translation of; report supersedes; old edition number, etc.

14. ABSTRACT. A brief (approximately 200 words) factual summary of the most significant information.

15. SUBJECT TERMS. Key words or phrases identifying major concepts in the report.

16. SECURITY CLASSIFICATION. Enter security classification in accordance with security classification regulations, e.g. U, C, S, etc. If this form contains classified information, stamp classification level on the top and bottom of this page.

17. LIMITATION OF ABSTRACT. This block must be completed to assign a distribution limitation to the abstract. Enter UU (Unclassified Unlimited) or SAR (Same as Report). An entry in this block is necessary if the abstract is to be limited.

(1) **Principle Investigator Name**: Mathew M. Maye

(2) **Grant/Contract Title:** *PECASE: New Synthetic and Assembly Methodology for Guiding Nanomaterial Assembly with High Fidelity into 1D Clusters and 3D Crystals Using Biomimetic Interactions*

(3) **Grant/Contract Number**: FA9550-10-1-0033

(4) **Reporting Period Start (MM/DD/YYYY)**: 01/01/2014

(5) **END (MM/DD/YYYY)**: 12/31/2014

(6) **Program Manager**: Dr. Hugh De Long

(7) **Annual Accomplishments (200 words maximum):** In year five of our grant we successfully completed a major grant milestone, and made progress and improvements in the areas where goals have previously been met. These accomplishments include: the first publication in the field on the self-assembly of quantum rods using DNA in which we used a patterned surface provided by DNA origami to control rod alignment and spacing (Section 1); published final results showing bioluminescence resonance energy transfer between firefly luciferase enzymes and rods that emit near infrared light (nIR), and improved long term stability and activity of the BRET nanoconjugates (Section 2). Finally, we completed a study that investigated ways to manipulate the 3D assembly of DNA-capped gold nanoparticles by using smart pH sensitive co-polymers, and transitioned that system to using elastin like polypeptides that have similar thermal- and pH responsive behavior (Section 3). We also successfully aquired and set-up an atomic force microscope purchased with AFOSR support. Two high impact articles were published, and one is in review. Four additional papers cite the grant, and three papers are in final stages of preparation.

(8) **Archival Publications (published) during reporting period:**

(1) *T.L. Doane*, R. Alam, **M.M. Maye*** *"Functionalization of Quantum Rods with Oligonucleotides for Programmable Assembly with DNA Origami"* *Nanoscale 2015, **7***, 2883-2888.

(2) R. Alam, L.M. Karam, *T.L. Doane,* J. Zylstra, D.M. Fontaine, B.R. Branchini, **M.M. Maye*** *"Near infrared bioluminescence resonance energy transfer from firefly luciferase-quantum dot bionanoconjugates"* *Nanotechnology* **2014**, 25, 495606.

(3) J. Gooch, A.A. Jalan, S. Jones, C.R. Hine, R. Alam, S. Garai, **M.M. Maye*,** A. Muller, J. Zubieta* "Keplerate cluster (Mo-132) mediated electrostatic assembly of nanoparticles" *J. Colloid Interface Sci.* 2014, 432, 144-150.

(4) C. M. Alexander, K. L. Hamner, **M.M. Maye***, J.D. Dabrowiak* "*Multifunctional DNA-Gold Nanoparticles for Targeted Doxorubicin Delivery*" *Bioconjugate Chem.* **2014**, 25, 1261-1271.

(5) S. Majumder, I.T. Bae, **M.M. Maye*** *"Investigating the role of polytypism in the growth of multi-shell CdSe/CdZnS quantum dots"* *J. Mater. Chem. C* 2014**, 2, 4659-4666**

(6) W. Wu, **M.M. Maye*** *" Discrete Dipole Approximation Analysis of Plasmonic Core/Alloy Nanoparticles"* *ChemPhysChem* **2014** (DOI: 10.1002/cphc.201402082).

(7) **Changes in research objectives (if any)**: This year we continued to use DNA origami as scaffolds upon which to assemble out quantum rods, which was not part of the original proposal. We note that it is not the goal of this project to develop new origami technology, but instead, to use it's capability to overcome some of the challenges we faced related to biomimetic patterning of nanomaterials. Using origami allowed us to achieve the state of the art in the field.

(8) **Change in AFOSR program manager, if any:** *n/a*

(9) **Extensions granted or milestones slipped, if any:** n/a

Section 0: Students, publications and presentations supported by this grant and those articles that cite the grant.

In this section we list all of the publications that were supported by the grant, and articles that cite the grant due to use of similar nanomaterials (i.e., qdots), common instrumenation or equipment as well as intellectual contributions. ***We thank the AFOSR for this transformational support.***

Students who were supported or participated on this project:

1. Dr. Hyunjoo Han (PhD 2012, now at Samsung, South Korea)
2. Dr. Colleen Alexander (PhD 2013, postdoc at UMass-Amherst, now at Bristol Myers Squibb)
3. Dr. Rabeka Alam (PhD 2013, now postdoc at Notre Dame)
4. Dr. Josh Zylstra (PhD 2013, now at ICON biotechnology)
5. Dr. Kristen Hamner (PhD 2014, now at Norwich Pharmaceuticals)
6. Dr. Tennyson Doane (Postdoc Fellow, 2013-present)
7. Dr. Jennifer Amey (Postdoc Fellow, 2010-2011, now at Binghamton University)
8. Kaitlin Coopersmith (PhD student)
9. Liliana Karam (PhD Student)
10. Alisha Lewis (PhD Student)
11. Yeutian Chen (Phd Student)
12. Simon Pun (undergrad B.S. '12)
13. Vallerie Valle (undergrad B.S. '11)
14. Nathanial Miska (B.S. '11, now NSF fellow at Brandeis)

Articles published or in final stages of submission:

1. *T.L. Doane*, R. Alam, **M.M. Maye*** *"Functionalization of Quantum Rods with Oligonucleotides for Programmable Assembly with DNA Origami"* ***Nanoscale 2015, 7,* 2883-2888.**
2. R. Alam, L.M. Karam, *T.L. Doane,* J. Zylstra, D.M. Fontaine, B.R. Branchini, **M.M. Maye*** *"Near infrared bioluminescence resonance energy transfer from firefly luciferase-quantum dot bionanoconjugates"* ***Nanotechnology* 2014**, 25, 495606.
3. K. Coopersmith, H. Han, M.M. Maye* *"Stepwise Assembly and Characterization of DNA Linked Two-Color Qdot Clusters"* ***Langmuir* 2015** (Submitted, ID #: la02015-01130u)
4. R. Alam*, L.M. Karam, T. Doane, D. Ablamsky, B. Branchini, M.M. Maye* *"Investigating the Origins of BRET efficiency in Luciferase modified Quantum Rod Nanosystems"* **2014** (In Submission)
5. K.L. Hamner, D. Smilgies, M.M. Maye* "*Small Angle X-ray Scattering Investigation of 3D Nanoparticle Assemblies with DNA and Thermosensitive co-Polymer Linkages*" *J. Phys. Chem. Lett.,* **2015** (In-Submission)
6. J. Gooch, A.A. Jalan, S. Jones, C.R. Hine, R. Alam, S. Garai, **M.M. Maye***, A. Muller, J. Zubieta* *"Keplerate cluster (Mo-132) mediated electrostatic assembly of nanoparticles"* J. Colloid Interface Sci. 2014, 15, 144-150.
7. C. M. Alexander, K. L. Hamner, **M.M. Maye***, J.D. Dabrowiak* "*Multifunctional DNA-Gold Nanoparticles for Targeted Doxorubicin Delivery*" ***Bioconjugate Chem.* 2014**, 25, 1261-1271.
8. S. Majumder, I.T. Bae, **M.M. Maye*** *"Investigating the role of polytypism in the growth of multi-shell CdSe/CdZnS quantum dots"* ***J. Mater. Chem. C* 2014**, 2, 4659-4666
9. W. Wu, **M.M. Maye*** *" Discrete Dipole Approximation Analysis of Plasmonic Core/Alloy Nanoparticles"* ***ChemPhysChem* 2014** (DOI: 10.1002/cphc.201402082).

10. H. Zang, P.K. Routh, **R. Alam**, **M.M. Maye**, M. Cotlet* *"Core size dependent hole transfer from a photexcited CdSe/ZnS quantum dot to a conductive polymer"* Chemical Communications 2014, 50, 5958-5960 [Cover Article]
11. Z. Xu, C. R. Hine, **M. M. Maye**, Q. Meng, M. Cotlet* *"Shell Thickness Dependent Photoinduced Hole Transfer in Hybrid Conjugated Polymer/Quantum Dot Nanocomposites: from Ensemble to Single Hybrid Level"* ***ACS Nano* 2012,** *6*, 4984–499
12. S. Srivastava, D. Nykypanchuk, **M.M. Maye**, A.V. Tkachenko, O. Gang* ***Soft Matter*** **2013** ,9, 10452-10457
13. K.L. Hamner, **M.M.Maye*** *"Thermal Aggregation Properties of Nanoparticles Modified with Temperature Sensitive Copolymers"* ***Langmuir 2013***, 29, 15217–15223
14. K.L. Hamner, C.M. Alexander, K. Coopersmith, *D. Reishofer, C. Provenza*, **M.M.Maye*** *"Using Temperature Sensitive Smart Polymers to Regulate DNA-Mediated Nanoassembly and Encoded Nanocarrier Drug Release"* ***ACS Nano* 2013**, *7*, 7011-7020.

Article 10 received *ChemComm* front cover.

15. W. Wu, **M.M. Maye*** *"Void Coalescence in Core/Alloy Nanoparticles with Stainless Interfaces"* ***Small* 2014, 10, 271-276.**
16. P. N. Njoki, W. Wu, P.S. Lutz, **M.M. Maye*** *"Growth Characteristics and Optical Properties of Core/Alloy Nanoparticles Fabricated via the Layer-by-Layer Hydrothermal Route"* ***Chemistry of Materials 2013*** 25, 3105-3113.
17. R. Alam, J. Zylstra, D. Ablamsky, B. Branchini, **M.M. Maye*** *"Novel Multistep BRET-FRET Energy Transfer using Nanoconjugates of Firefly Proteins, Quantum Dots, and Red Fluorescent Proteins"* ***Nanoscale*** **2013**,**5**, 5303-5306
18. **M.M. Maye*** *"Self-Assembly: En Route to patchy superlattices"* *Nature Nanotechnology* **2013**, *8*, 5-6. (News & Views Review)
19. H. Han, *V. Valle,* **M.M. Maye*** *"Probing Resonance Energy Transfer and Inner Filter Effects in Qdot – Large Metal Nanoparticle Clusters using a DNA-mediated Quench and Release Mechanism"* ***Journal of Physical Chemistry C* 2012** *116*, 22996-23003
20. P.N. Njoki, P. Lutz, W. Wu, *L. Solomon*, **M.M. Maye*** *"Exploiting Core/Shell and Core/Alloy Interfaces for Asymmetric Growth of Nanoparticles"* ***Chem. Commun.***, 2012,**48**, 10449-10451
21. R. Alam, D. Ablamsky, B. Branchini, **M.M. Maye*** *"Designing Quantum Rods for Optimized BRET with Firefly Luciferase Enzymes"* ***Nano Letters 2012,*** *12*, 3251-3156.
22. C. Alexander, J. Dabrowiak,* **M.M. Maye*** "Investigation of the Drug Binding Properties and Cytotoxicity of DNA-Capped Nanoparticles Designed as Delivery Vehicles for the Anticancer Agents Doxorubicin and Actinomycin D" ***Bioconjugate Chemistry* 2012** 23, 2061–2070.
23. J. Zylstra, H. Han, R. Alam, R.P. Doyle, **M.M. Maye*** *"Tailoring Quantum Dot Interfaces for Improved Biofunctionality and Energy Transfer"* ***ACS Symposium Series*, 2012, 1112, 59-79.**
24. H. Han, *V. Valle,* **M.M. Maye*** *"Probing the quenching of CdSe/ZnS qdots by Au, Au/Ag, and Au/Pd Nanoparticles"* ***Nanotechnology* 2012 23** 435401
25. P.N. Njoki, W. Wu, H. Zhao, *L. Hutter*, E. A. Schiff, **M.M. Maye*** "*Layer-by-Layer Processing and Optical Properties of Core/Alloy Nanostructures"* ***J. Am. Chem. Soc.*, 2011**, *133*, 5224–5227(Communication)
26. P.N. Njoki, *L. Solomon*, W. Wu, R. Alam, **M.M. Maye*** *"Attenuating Surface Plasmon Resonance using Core/Alloy Architectures"* ***Chem. Commun.* 2011,** *47*, 10079-00081
27. W. Wu, P.N. Njoki, H. Han, H. Zhao, E. A. Schiff, P. S. *Lutz, L. Solomon, S. Matthews,* **M. M. Maye*** *"Processing Core/Alloy/Shell Nanoparticles: Tunable Optical Properties and Evidence for Self-Limiting Alloy Growth"* ***J. Phys. Chem. C*, 2011**, *115*, 9933–9942.
28. H. Han, J. Zylstra, **M.M. Maye*** *"Direct Attachment of Oligonucleotides to Quantum Dot Interfaces"* ***Chem. Mater.* 2011**, 23, 4975–4981

29. R. Alam, **M.M. Maye*** *"Asymmetric Quantum Dot Growth via Temperature Cycling"* ***Inorganica Chimica Acta*** **2012,** *380*, 114-117.
30. C. M. Alexander, **M. M. Maye*,** J. C. Dabrowiak* "*DNA-capped nanoparticles designed for doxorubicin drug delivery"* ***Chem. Commun.,*** **2011**, *47*, 3418-3420.
31. J. Zylstra, J. Amey, *N. J. Miska*, *L. Pang*, C. R. Hine, *J. Langer*, R. P. Doyle, **M. M. Maye*** *"A Modular Phase Transfer and Ligand Exchange Protocol for Quantum Dots"* ***Langmuir,*** **2011**, *27*, 4371–4379.
32. H. Han, *G. Di Francesco*, **M.M. Maye*** *"Size Control and Photophysical Properties of Quantum Dots Prepared via a Novel Tunable Hydrothermal Route"* ***J. Phys. Chem. C*** **2010**, *114*, 19270.
33. H. Han; *G.N. Di Francesco*, *A. Sexton*; *A. Tretiak*, **M.M. Maye*** ***Mater. Res. Soc. Symp. Proc. Vol. 1220,*** **2010,** 12220-BB03-02

Presentations by PI and staff that cited grant

1. **M.M. Maye** "Nanomaterials" 2015 Keynote Address, Central New York Science & Engineering Fair (CNYSEF), Onondaga Community College, MOST Museum, March 22, 2015.
2. **M.M.Maye** *"Designing Nanomaterial Architectures for Applications in Self-Assembly, Drug-Delivery, and Energy Transfer"* ACS Susquehanna Valley Section Lecture, March 12, 2014, Susquehanna Univ.
3. **M.M. Maye**, "UMRI Alumni: From UMRI to PECASE, The Power of Undergraduate Research In Materials Science" (AAA5.04) MRS Fall Meeting, Boston Mass. 2014
4. **M.M. Maye**, K. Hamner, J. Tinklepaugh, S. Pun, D. Smilgies, "Using Smart Polymers to Regulate DNA-Mediated Nanoparticle Assembly, Crystal Formation, and Interparticle Spatial Properties" MRS Fall Meeting, Boston Mass. 2014
5. **K. Coopersmith**, A. Lewis, L. Karam, M.M. Maye, "The DNA-Mediated Assembly and Purification of Multi-Color Qdot Clusters" (JJ3.11) MRS Fall Meeting, Boston Mass. 2014
6. **A. Lewis**, T.L. Doane, K. Coopersmith, M. Bowick, M.M. Maye, "Using Kinetics and Ultracentrifugation to Prepare and Collect Nanoparticle Clusters Assembled via DNA Mediated Approaches" (JJ3.10) MRS Fall Meeting, Boston Mass. 2014
7. **T.L. Doane**, M.M. Maye, "Assembly and Aligning of Semiconductive Quantum Rods onto DNA Origami Substrates" (KK7.01) MRS Fall Meeting, Boston Mass. 2014
8. **T.L. Doane**, M.M. Maye, "Assembly and Aligning of Semiconductive Quantum Rods onto DNA Origami Substrates" Gordon Research Conference, 2014
9. **A. Lewis**, T.L. Doane, K. Coopersmith, M. Bowick, M.M. Maye, "Organizing Quantized Clusters of Nanoparticles by Fine Tuning Self-Assembly Kinetics in a DNA-Mediated Self-Assembly System" Syracuse Biomaterials Institute Stevensen Lecture Poster Session, October 2014
10. **J. Tinklepaugh**, M.M. Maye, "Functionalization of Nanoparticles with Smart Polymers for Controllable Self-Assembling Systems" Syracuse Biomaterials Institute Stevensen Lecture Poster Session, October 2014
11. **K. Coopersmith**, M.M. Maye, "The DNA Mediated Assembly and Ultracentrifugation Based Purification of Multi-Color Qdot Clusters" Syracuse Biomaterials Institute Stevensen Lecture Poster Session, October 2014
12. **K. Hamner** "Using Temperature-Sensitive Smart Polymers to Regulate DNA-mediated Nano Assembly" PhD Defense, July 25, 2014.
13. **K. Hamner**, D. Smilgies, M.M. Maye *"Small angle X-ray scattering study of interparticle spatial properties of nanoparticles assembled by DNA and thermosensitive co-polymers"* ACS Fall Meeting, Colloids/Nanoscience Section, Indianapolis, 2013
14. **P. Lutz**, W. Wu, M.M. Maye *"Controlling composition, asymmetry, and internal microstructure of nanomaterials using a core/alloy approach"* **ACS Fall Meeting**, Colloids/Nanoscience & Sci-Mix Section, Indianapolis, 2013
15. **S. Majumder,** M. M. Maye *"Investigating the role of polytypism in the growth of multishell CdSe/CdZnS quantum dots"* **ACS Fall Meeting**, Colloids/Nanoscience Section, Indianapolis, 2013
16. **K. Coopersmith**, R. Davon Slaton, H. Han, M.M. Maye *"Stepwise assembly of multicolor qdot clusters using a DNA-mediated approach"* **ACS Fall Meeting** Fundamental Research in Colloid and Surface Science.
17. **K. Hamner**, D. Smilgies, M.M. Maye *"Small angle X-ray scattering study of interparticle spatial properties of nanoparticles assembled by DNA and thermosensitive co-polymers"* Cornell CHESS User Meeting July 2013.
18. **K. Hamner**, M.M. Maye "Using Smart-Polymers to Regulate Nanoparticle Assembly" Programmable Self-Assembly of Matter" conference, ICAM-I2CAM @ NYU **awarded best poster, sponsored by Nature Materials.
19. **K. Coopersmith**, R. Davon Slaton, H. Han, M.M. Maye *"Stepwise assembly of multicolor qdot clusters using a DNA-mediated approach"* Syracuse Biomaterials Institute (SBI) Stevenson Lecture Poster Session, Nov 2013.
20. **R. Alam**, D.M. Fontaine, B.R. Branchini, M.M. Maye "Designing Quantum Rod Morphology and Surface Chemistry for Optimum Bioluminescence Resonance Energy Transfer" **MRS Spring Meeting**, San Francisco, LL6: Biomaterials II
21. **W. Wu**, M.M. Maye "Controllable Vacancy Coalescence in Core/Alloy Nanoparticles" **MRS Spring Meeting**, San Francisco, L6: Nanoparticle Manufacturing.

22. **K. Hamner**, M.M. Maye "Using Smart-Polymers to Regulate Nanoparticle Assembly" Central New York Biotechnology Symposium, May 2013
23. **K. Coopersmith**, R. Davon Slaton, H. Han, M.M. Maye *"Stepwise assembly of multicolor qdot clusters using a DNA-mediated approach"* Central New York Biotechnology Symposium, May 2013
24. **M.M. Maye** "Designing Quantum Rod Morphology, Microstructure, and Surface Chemistry for Optimum Energy Transfer" Colloquia, SUNY-Albany Chemistry Department & Nanoscience Institute, Oct 2013.
25. **M.M. Maye** "From Design To Construction: Nanomaterials with Tailored Optics, Microstructure, Morphology, and Energy Transfer Ability" Colloquia, Connecticut College, Department of Chemistry, Oct 2013.
26. **M.M. Maye** "Designing Quantum Rod Morphology, Microstructure, and Surface Chemistry for Optimum Energy Transfer CLEO Optics Meeting, San Jose, June 2013
27. **M.M. Maye** *"Bioluminescence Resonance Energy Transfer Between Quantum Rods and Firefly Luciferase"*
28. MRS Spring Meeting, LL8: Hybrid Inorganic-Biological Materials, April 2013.
29. **M.M. Maye** *"Controlling Composition, Asymmetry, and Internal Microstructure of Nanomaterials Using a Core/Alloy Approach"* M14: Nanoparticles, Nanorods, Quantum Dots and Nanocrystals III April 2013
30. **M.M. Maye** "Bioinspired Self-Assembly and Energy Transfer Using Nanomaterials" Syracuse Center of Excellence (COE) Biomimetics Day
31. **M.M. Maye** *"Bioinspired Self-Assembly and Energy Transfer Using Nanomaterials"* **Syracuse University, Department of Physics Colloquia, November 2012.**
32. **M.M. Maye** *"From Design to Construction: Nanomaterials with Tailored Optics, Microstructure, Morphology, Optics, and Energy Transfer Ability"* **Syracuse University, Department of Chemistry Colloquia, September 2012**.
33. **M.M. Maye**, R. Alam, "Designing Quantum Rod Morphology and Surface Chemistry for Optimum Energy Transfer" **Brookhaven National Lab, Center for Functional Nanomaterials Department, Colloquia, July 2012.**
34. **M.M. Maye**, P. Njoki, W. Wu, P. Lutz *"Synthesis and Optical Properties of Core/Alloy Nanoparticles"* (PHYS: Synthesis, Spectroscopy, Theory and Applications of Nanocrystals and Nanowires, #122) **244th ACS Meeting, 2012, Philadelphia**
35. **M.M. Maye,** C. Alexander, J. C. Dabrowiak *"DNA-capped nanoparticles as encoded nanocarriers for intercalating chemotherapy drugs"* (COLL: Functional Nanoparticles for Biomedical Application, #193) **244th ACS Meeting, 2012, Philadelphia**
36. **M.M. Maye** *"Soft macromolecule and biomacromolecules functionalized nanoparticles for tailored self-assembly"* (COLL: Half a Century of Fine Particles Science, #156/Invited) **244th ACS Meeting, 2012, Philadelphia**
37. **M.M. Maye**, R. Alam, B.R. Branchini, D.M. Fontaine, H. Han, J. Zylstra " *Bioluminscence resonance energy transfer between quantum rods and firefly luciferase"* (COLL: Abiotic/Biotic Interfaces) **244th ACS Meeting, 2012, Philadelphia**
38. **M.M. Maye**, *"Nanoparticle Nanotechnology: Synthesis, Processing, and Biomimetic Assembly"* **Clarkson University, Chemistry Department Colloquia, January 27, 2012**
39. **M.M. Maye**, *"Nanoscience: Exploring Big Ideas by Organizing the Smallest of Matter"* **Binghamton University, Materials Research Department, MRS Nano-Days Keynote Lecture, March 27, 2012**
40. **R. Alam**, H. Han, M.M. Maye *"Correlating Energy Transfer Efficiency with Quantum Rod Composition, Aspect, Ratio, and Microstructure in Biotic-Abiotic Nanosystem"* **DOE Joint NSRC Workshop on Nanoparticle Science, November 5-6, 2012, DOE Argonne National Laboratory**
41. **J. Zylstra,** R. P. Doyle, M. M. Maye *"Phase transfer and biofunctionalization of Quantum dots via the histidine mediated phase transfer method."* **ACS Northeast Region Meeting (NERM), #68, 2012, Rochester NY**.
42. **R. Alam**, M.M. Maye *"Asymmetric quantum dot and quantum rod growth via temperature cycling" (*INOR: Nanoscience, #539) **ACS Northeast Region Meeting (NERM), #70, 2012, Rochester NY**.
43. **R. Alam**, D.M. Fontaine, B.R. Branchini, **M.M. Maye** *"Designing quantum rod morphology and surface chemistry for optimum energy transfer"* **ACS Northeast Region Meeting (NERM), #182, 2012, Rochester NY**.
44. **W. Wu**, M.M. Maye *"Modeling the optical properties of core/alloy nanoparticles via discrete dipole approximation"* **ACS Northeast Region Meeting (NERM), #183, 2012, Rochester NY**.

45. **R. Alam**, M.M. Maye *"Asymmetric quantum dot and quantum rod growth via temperature cycling" (*INOR: Nanoscience, #539) **244th ACS Meeting, 2012, Philadelphia**
46. **R. Alam**, D.M. Fontaine, B.R. Branchini, **M.M. Maye** *"Designing quantum rod morphology and surface chemistry for optimum energy transfer"* (PHYS: Poster Session, #382) **244th ACS Meeting, 2012, Philadelphia**
47. **W. Wu**, M.M. Maye *"Modeling the optical properties of core/alloy nanoparticles via discrete dipole approximation"* (PHYS: Poster Session, #377) **244th ACS Meeting, 2012, Philadelphia**
48. **M. Maye,** *"A Modular Phase Transfer and Biomimetic Assembly Protocol for Quantum Dots",* (Biological Hybrid Materials for Life Sciences, #JJ5.5), 2011 Spring MRS Meeting, **2011**, San Francisco
49. **M. M. Maye**, J. Zystra, H. Han, R. Alam, V. Valle, *"Direct bioattachent to Qdot interfaces for short FRET distances",* (Colloids, #330), 242nd ACS Meeting, **2011**, Denver
50. **M. M. Maye**, P. N. Njoki, W. Wu, L. Solomon, P. Lutz, R. Alam, *"Fine-tuning surface plasmon resonance using core/alloy and core/alloy/shell architectures",* (Phys, #319) 242nd ACS Meeting, **2011**, Denver
51. **M. M. Maye**, J. C. Dabrowiak, C. M. Alexander, "DNA-capped nanoparticles designed for doxorubicin drug delivery" (Colloids, #284) 242nd ACS Meeting, **2011**, Denver
52. **M. M. Maye**, J. Zylstra, H Han, C. Alexander, J. Dabrowiak, R. P. Doyle, *"Developing modular surface chemistry approaches for biological and drug loading at nanoparticle interfaces"* (Biocolloids and Biological Interfaces-I, #10) 85th ACS Colloids and Surface Science Symposium, **2011**, Montreal
53. **M. M. Maye**, P. N. Njoki, W. Wu, *"Exploring nanoparticle phase behavior using core/alloy/shell and core/alloy models"* (Synthesis of Nanostructures and Surface Science II, #79) 85th ACS Colloids and Surface Science Symposium, **2011**, Montreal
54. **M. M. Maye**, H. Han, C. R. Hine, R. Alam, P. N. Njoki, *"Investigation of Hydrothermally Processed Nanomaterials for Integration with Third Generation Photovoltaics"* **2011** NSLS-CFN User Meeting.
55. **M. M. Maye**, H. Han, C. R. Hine, R. Alam, P. N. Njoki, *" Hydrothermal Processing Quantum Dots and Alloy Nanoparticles"* DOE BES Scientific User Facilities Division E-Beam Microcharacterization Centers and Nanoscale Science Research Centers 2011 Contractors' Meeting. 2011, Annapolis
56. **M.M. Maye**; *"3D Crystalline Organization in DNA-Mediated Nanoparticle Assemblies":* Cornell, Cornell High Energy Synchrotron Source (CHESS), Invited Colloquia.
57. **M.M. Maye**; *"Single Molecule Observation of PL Enhancement in Qdot Nanoparticle Heterodimers"* Picoquant Workshop #5: "Making single molecule fluorescence lifetime easier" BNL/CFN, Invited Talk.
58. **M.M. Maye** "*Quantum Dots for Sensing and Bioimaging*." 2010 NERM ACS (Nano, #155), Invited Talk.
59. **M.M. Maye**, H. Han, C.R. Hine, G.N. Di Francesco, L. Solomon, P. Lutz, Synthesis of Plasmonic Nanoparticles and Quantum Dots via Hydrothermal Method" 239th ACS-Meeting, Boston, MA (#1162)
60. **J. Zylstra**, N. Miska, M.M. Maye "Modular phase transfer and ligand exchange protocol for quantum dots" 240th ACS-Meeting, Boston, MA (Colloids & Surf, #258)
61. **H. Han**, P. Lutz, M.M. Maye "Synthesis of core-shell quantum dots via MAPS for Biofunctionalization" ACS-Meeting, Boston, MA (Colloids & Surf, #257)
62. **C. Hine**, A. Roy, M.M. Maye New insights into ligand effects during quantum dot nucleation and growth, 240th ACS-Meeting, Boston, MA (Physical Chemistry, #590)

Section 1: Using DNA Mediated assembly to organize quantum rods and metal nanoparticles for future energy transfer and optics control (COMPLETED)

Personnel: Dr. Tennyson Doane (Postdoc Fellow), Kaitlin Coopersmith (summer RA), Alisha Lewis (unsupported grad student, NSF IGERT Fellow)

Months : Jan-Dec 2014

Publications from Grant*:*

1. T.L. Doane, R. Alam, M.M. Maye* *"Functionalization of Quantum Rods with Oligonucleotides for Programmable Assembly with DNA Origami"* ***Nanoscale 2015, 7,*** **2883-2888.**
2. K. Coopersmith, H. Han, M.M. Maye* *"Stepwise Assembly and Characterization of DNA Linked Two-Color Qdot Clusters"* ***Soft Matter*** **2015**, (Submitted Dec '14: ID SM-COM-12-2014-002908), now at ***Langmuir*** **2015** (Submitted, ID #: la02015-01130u)

Presentations*:*

- **T.L. Doane**, M.M. Maye, "Assembly and Aligning of Semiconductive Quantum Rods onto DNA Origami Substrates" (KK7.01) MRS Fall Meeting, Boston Mass. 2014
- **T.L. Doane**, M.M. Maye, "Assembly and Aligning of Semiconductive Quantum Rods onto DNA Origami Substrates" Gordon Research Conference, 2014
- **M.M.Maye** *"Designing Nanomaterial Architectures for Applications in Self-Assembly, Drug-Delivery, and Energy Transfer"* ACS Susquehanna Valley Section Lecture, March 12, 2014, Susquehanna Univ.
- **M.M. Maye**, "UMRI Alumni: From UMRI to PECASE, The Power of Undergraduate Research In Materials Science" (AAA5.04) MRS Fall Meeting, Boston Mass. 2014
- **K. Coopersmith**, M.M. Maye, "The DNA Mediated Assembly and Ultracentrifugation Based Purification of Multi-Color Qdot Clusters" Syracuse Biomaterials Institute Stevenson Lecture Poster Session, October 2014
- **A. Lewis**, T.L. Doane, K. Coopersmith, M. Bowick, M.M. Maye, "Organizing Quantized Clusters of Nanoparticles by Fine Tuning Self-Assembly Kinetics in a DNA-Mediated Self-Assembly System" Syracuse Biomaterials Institute Stevenson Lecture Poster Session, October 2014
- **A. Lewis**, T.L. Doane, K. Coopersmith, M. Bowick, M.M. Maye, "Using Kinetics and Ultracentrifugation to Prepare and Collect Nanoparticle Clusters Assembled via DNA Mediated Approaches" (JJ3.10) MRS Fall Meeting, Boston Mass. 2014
- **K. Coopersmith**, A. Lewis, L. Karam, M.M. Maye, "The DNA-Mediated Assembly and Purification of Multi-Color Qdot Clusters" (JJ3.11) MRS Fall Meeting, Boston Mass. 2014
-

Summary: In this section we describe our work related to DNA-mediated assembly of nanomaterials. This year we focused entirely on the self-assembly of quantum rods (QRs) onto DNA origami supports. Here, we use DNA origami solely as a nano-scale patterning tool, and did not focus on new origami science. The purpose of this project was to assemble multiple QRs onto the origami with controlled QR spacing and orientation. We succeeded in improving our assembly yields (compared to early data in year 4), as well as in developing new ways to purify the QR+Origami conjugates, which we achieved using gradient ultracentrifugation. The results demonstrate our ability to assemble two QR per origami that can have the same or varied fluorescence colors. We probed energy transfer between the rods and also the role of origami flexibility on self-assembly efficiency. This final study is the result of a five-year evolution from the original goals of the project, which was to assemble spherical quantum dots (QDs) into controlled clusters. *The primary goals* of this section were to; (*i*) demonstrate the ability to assemble and disassemble multi-color qdots clusters using DNA-mediated interactions and to study FRET between Qdots (***goals achieved in year 1-2, &5***), (*ii*) to extend the approach towards Qdot-NP clusters (***goals achieved in year 3***), to (*iii*) explore the energy transfer capability in the nanostructured assemblies using quantum rods (***objectives transitioned in year 4***), and (*iv*) to ultimately assemble these QDs (or QRs) in a rational fashion at a solid-support (***goals achieved this year, year 5)***

Overview: This year we finished our investigation of using DNA mediated interactions to self-assemble CdSe/CdS quantum rods (QRs). As briefly introduced last year, we explored the use of simple DNA origami to organize the spatial properties of the rods. ***We note that in our project, the goal is not to spend resources designing new and elaborated origami, but instead simply to use it as a nano-scale patterning tool to organize the rods***. Using DNA origami allows us too overcome challenges in aligning of nanomaterials. We made a number of significant advances this year, including the successful modification of the QRs with DNA, the assembly of one QR assembly orientation, as well the development of new ways to purify the assemblies via gradient ultracentrifugation.

This project (Section 1) was the primary focus of year 5 of our grant, and ~80% of the yearly budget went towards this project. This included the support of the postdoctoral fellow, the materials and supplies, as well as the purchase of an AFM and Ultracentrifuge. The former of which was possible because of students graduating and not being on RA or summer support in year 4.

As we have describe before in previous reports, semiconductive quantum rods (QRs) are an interesting class of nanomaterial because of composition and size tunable optoelectronic properties, as well as morphology and microstructure derived optical polarization. This is particularly true for colloidal II-IV core/shell QRs, like CdSe/CdS, where the core shape is responsible for polarized emission, which can be further sensitized by the shell. Harnessing QR polarization may lead to advances in colloidal lasing, optical filtering, and energy transfer, especially between two or more different QR types with similar polarized optical properties. For example, QRs with rod-in-rod microstructure show linearly polarized emission, which has shown importance in non-radiative energy transfer processes with dyes and biomolecules. Thus, by organizing such rods into unique architectures, new collective optoelectronic properties may be possible. However to achieve this, QRs need to be assembled with controlled orientation and spacing to maximize optical interactions. Approaches for aligning QRs are varied, and include: manipulating inter-particle depletion forces, mechanical treatment after polymer immobilizations, and electrophoretic deposition. These techniques, however, are generally utilized for a single QR type (i.e. color), and form dense macroscopic structures.

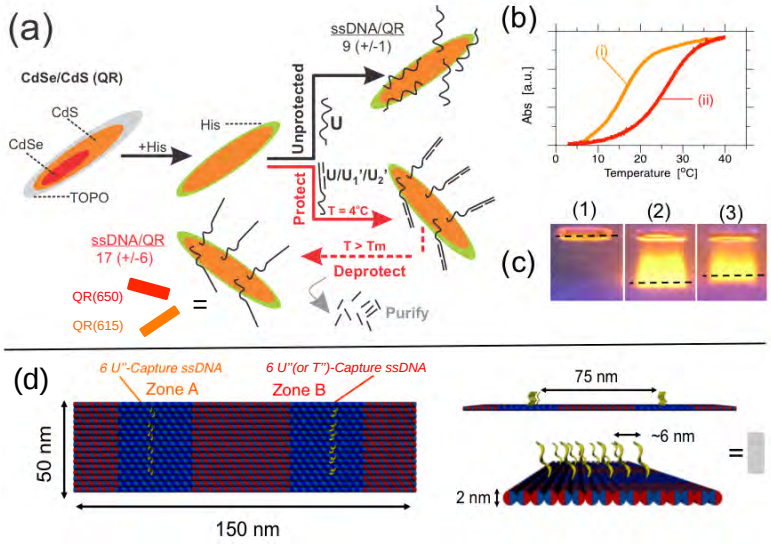

Figure 1: (a) Schematic of the DNA functionalization strategy. (b) Thermal denaturation profiles for *U/U'$_1$/U'$_2$* (i) and *T/T'$_1$/T'$_2$* (ii). (c) A 0.5% agarose gel image of His-QR (1), *U*-QR (2), and *U/U'$_1$/U'$_2$*-QR (3). (d) Illustration of origami substrate assembly highlighting assembly zones.

Thus, one under studied and potentially lucrative area of QR research is the development of new approaches for pre-programmed alignment of discrete multi-QR structures, where QR stoichiometry, order, and orientation can be controlled.

To address this limitation, we studied a combination of two DNA-mediated bottom-up routes; (i) the synthesis of QRs and the modification with single stranded DNA (ssDNA), and (ii) the design and assembly of DNA origami to organize alignment. Here, the goal of our project is not to focus on new origami designs, but instead to use the origami as a patterning tool to organize the QRs with precision not available using other soft-lithography techniques. To the best of our knowledge, our project, and the paper published this year, is the first report to focus on functionalization of QRs with DNA, as well as assembly on origami. This work was published in *Nanoscale* this year.

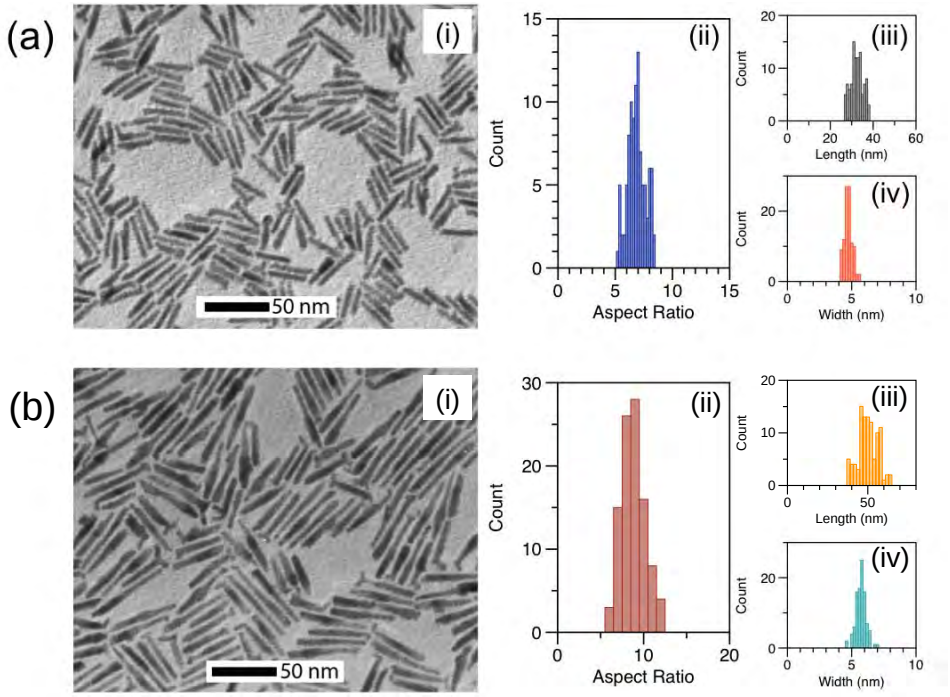

Figure 2. TEM images (i) of QR(615) (a) and QR(650) (b) with statistical analysis (ii-iv). The QR(615) have an average l/w = 6.8 ± 0.8 (l = 32.3 ± 2.9 nm, w = 4.7 ± 0.3 nm) and the QR(650) have an average l/w = 8.8 ± 1.4 (l = 50.1 ± 6.1 nm, w = 5.7 ± 0.4 nm).

Figure 1a shows the strategy employed to first modify the QR with ssDNA. To start, a QR with an aspect ratio of l/w = 6.8 ± 0.8 (l = 32.3 ± 2.9 nm, w = 4.7 ± 0.3 nm, Fig. S1) that emitted at 615 nm (denoted as QR(615), Fig. S2) was synthesized, and phase transferred to borate buffer (10 mM, pH = 8.0) using the histidine (His) mediated phase transfer method developed in year 2 of our project (see previous reports). These His-modified QRs were then modified with ssDNA using two approaches. In the first, a 30-b ssDNA (denoted as *U*-type, Table S1) that was modified with six 5'-phosphorothioate bases were incubated with the QR solution at a molar ratio of [ssDNA]:[QR] = 128 ([QR] = 1mM) for 3-5h, followed by salt aging and purification. The number of active *U* per QR was quantifying by hybridization with Cy3 modified complementary strands, and determined that 9 ± 1 *U* per QR was a typical coverage. Early assembly studies using these *U*/QR were unsuccessful, and we speculated that a factor was low DNA coverage, the result of non-specific ssDNA interactions and coordination to the Cd^{2+} rich interface, which would render them inactive in assembly.

To overcome this challenge, a simple protection/deprotection strategy was developed. To "protect" the *U*-ssDNA, it was first partially hybridized by two short complementary strands, 7-b U'_1 and 8-b U'_2. Short strands were chosen to ensure low denature temperatures (Tm), which in turn, could be used to "deprotect" the system later at T > Tm. Figure 1b shows the thermal denaturation behavior of the protected $U/U'_1/U'_2$ which showed a T_m transition at 16 °C. The protected $U/U'_1/U'_2$ were then incubated with the QRs at 4 °C under the same conditions as above. The resulting conjugates were then purified free of excess ssDNA by first raising the temperature to 25 °C, thus denaturing the $U/U'_1/U'_2$, and then centrifugation based precipitation of the QRs, followed by subsequent removal of the ssDNA containing supernatant. This step resulted in an increase in the ssDNA coverage to 14 - 17, and the QRs used in this study had 17 ± 6 *U*/QR. This coverage increase was observed by agarose gel electrophoresis (Fig. 1c), which revealed slower mobility for the protected *U*/QR sample (lane 3), which is attributed to both increased hydrodynamic diameter (D_h), the result of both the increased number coverage and less wrapping. It is worth noting that considering the surface area of the QRs, this improved coverage is still ~3x lower than the expected maximum when using a single thiol ssDNA model. However, considering that the *U*-ssDNA had a five base phosphorothioate linkage to the interface, these values are likely near saturation for our conditions. As the protected system led to improved ssDNA coverage and assembly kinetics, we focused solely on that approach to prepare QRs for subsequent assembly steps.

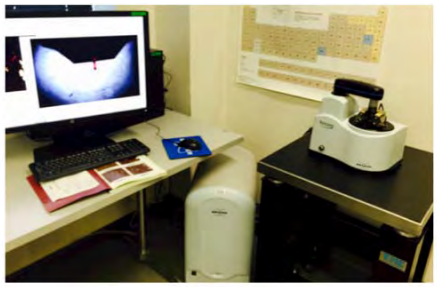

Bruker Innova SPM purchased this year via grant funds.

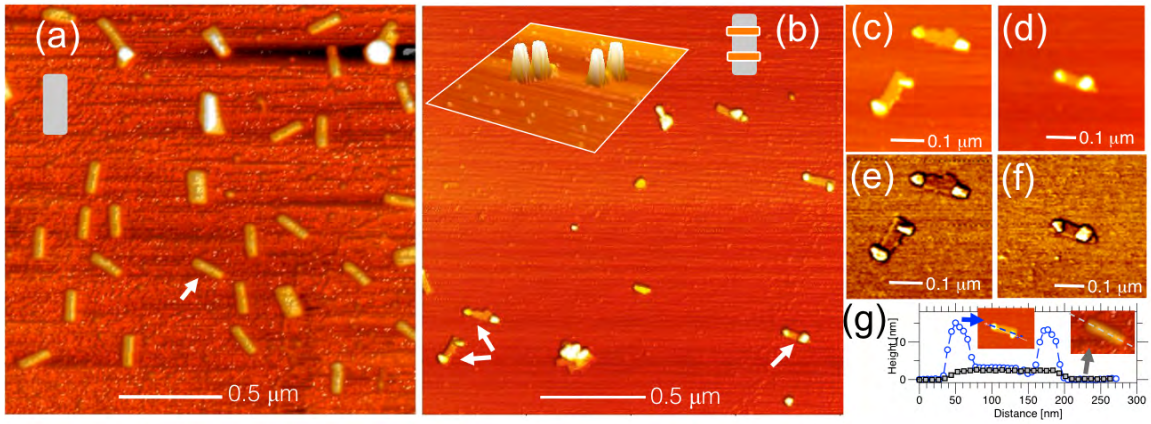

Figure 3: (a) Representative AFM height image of origami substrates deposited on mica. (b) AFM images of *U*/QR + origami assemblies after self-assembly in solution and then casting onto mica. Inset shows additional region of surface in 3D. (c-f) Zoomed images corresponding to the arrows in b and imaged in both height (c-d) and phase (e-f) mode, distinguishing QR from origami in phase images. (g) Cross-section analysis of origami and QR+origami assemblies for inserted images.

The *U*/QR were then assembled onto novel DNA origami designed to allow spatial control and alignment of the QRs. Figure 1d shows a schematic of the origami that was designed, and was based on M13mp18 circular ssDNA and 212 staple strands (see Appendix 1). The origami is rectangular, measuring approximately 155 X 55 nm, is one duplex thick, and has five distinct zones, two of which (Zone A and Zone B) are designated as QR capture zones. In these zones, six complementary *U''* ssDNA capture strands extend from the surface, with ~ 6 nm distance between strands. Figure 2a shows a typical AFM height image, where the rectangular origami can be observed. The dimensions obtained by taking a cross-section of the images (see overlay of Fig. 2g) were in good agreement with the predicted values. Some small features on the mica surface are attributed to excess staple strands or partial assemblies that persisted after purification.

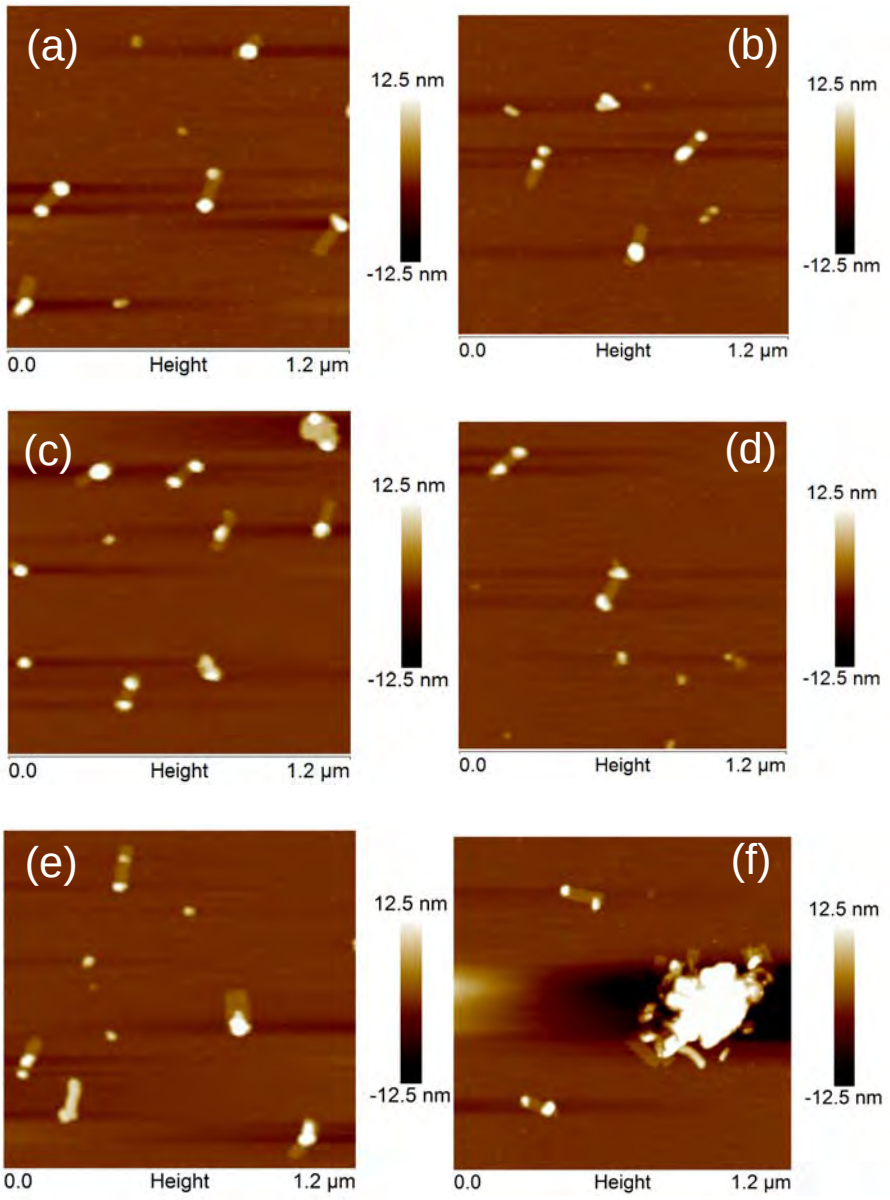

Figure 4. Additional AFM images of U_{Rigid}-QR(615)-origami conjugates. Statistical analysis found that 70% of origami contained at least one rod, with 29% having two per origami (N =148) after 2.5 hr incubation.

Next, these origami were suspended in solution and incubated with *U*-QRs at a 50 fold QR excess for 1-24 h at room temperature in 100 mM NaCl – 10 mM Tris Acetate. After assembly, the crude assembly solution could be cast on mica and imaged. Figure 2b is a typical AFM height image for the QR+origami conjugates. As can be observed in the image, the substrates now have raised height features located at the regions close to the two assembly zones. Additional zoomed images in both height (c-d) and phase imaging mode (e-f) are shown, the latter of which suggests the raised features are significantly harder (higher contrast), indicating the inorganic QRs. Further analysis across many sample regions reveal the presence of both mono- and bi-functionalized substrates, as well as the presence of low populations of free QRs. Additional AFM images are shown in Figure 4. Height analysis of the QR+origami (Figure

2g), showed that the raised features are 8~12 nm, which is consistent with the dimensions of the width of the *U*/QRs after considering rod diameter and dried DNA length.

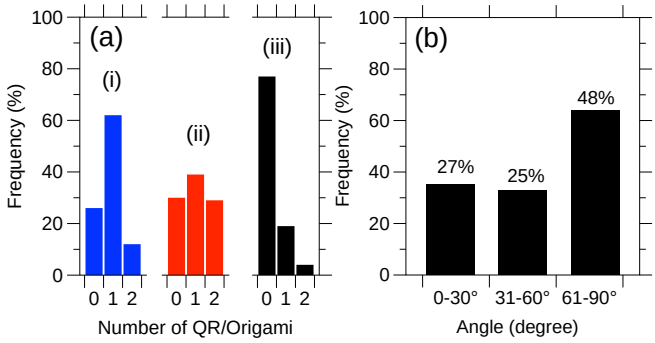

Figure 5: Statistical analysis of AFM images quantifying (a) the assembly stoichiometry after 1.0 (i, *n* = 99) 2.5 (ii, *n* = 98) and 24 h assembly times (iii, *n* = 104); and (b) the angle of orientation for the assembled QR with respect to the origami long axis (*n* = 142).

The assembly yields, stoichiometry, and relative angle of QR assembly could then be studied from the AFM results. For example, Figure 5a shows the results of statistical analysis of assembly stoichiometry. After 1h of assembly (i), over 70% of the origami had at least one QR (mono-functionalized), with 12% having two (bi-functionalized). At 2.5h these values increased to 30% bi-functionalized. Although assembly times approaching 24 hours have been reported to improve hybridization efficiency, the same experiment in this system resulted in a surprising decrease in assembly efficiency, which is possibly due to the agglomeration of the functionalized structures. These values are for a typical case, which includes each assembly zone having 6 capture strands. Interestingly, the bi-functional population could be consistently increased to ~30% by first making the spacer region of the *U* rigid (denoted as U_{Rigid}, Table 1), as shown in Fig. 4. As described above, the origami design was intended to align the QRs in Zone A and B in parallel for this proof-of-principle study. Figure 5b shows the results of the analysis of QR alignment, as collected from many AFM micrographs of the U_{rigid} assembly system. The results indicate 48% of the QRs were angled between 61-90^{o} to the origami long axis (Fig. 5b), as measured by determining the long axis of the QR heights.

Table 1: ssDNA strands used in this study, see appendix 1 for origami sequences

Type	Sequence (* = Phosphorothioate bases)	T_m $S/S'_1/S'_2$ (°C)
U	T*T*T* T*T*T TTT TTA CTC ACC TAT ATC A	
U'_1	GTG AGT A	16.5
U'_2	TGA TAT AG	
U'_3	TGA TAT AGG TGA GTA	
U_{Rigid}	G*G*G* G*G*T TTT TTT TTT TTT TTT ACT CAC CTA TAT CA	
T	T*T*T* T*T*T TTT TTC ACG ACA CAC TTT G	
T'_1	GTC GTG A	27
T'_2	CAA AGT GT	
T'_3	CAA AGT GTG TCG TGA	

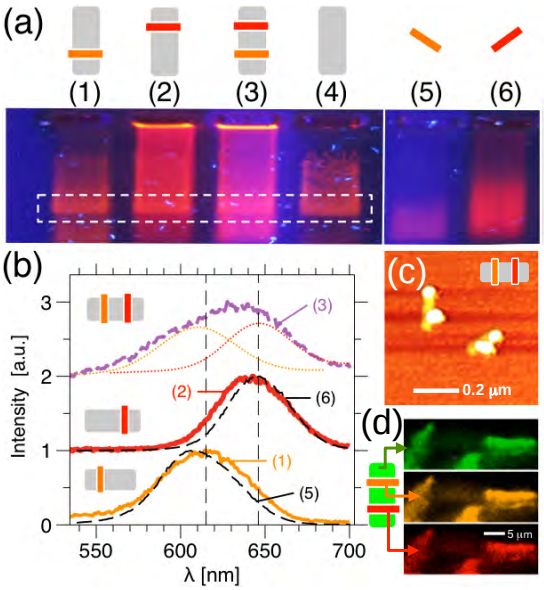

Figure 6: (a) Gel electrophoresis of the dual capture substrate after assembly with (1) U/QR(615), (2) T/QR(650), (3) both QRs, and the (4) substrate alone, as well as free (5) U/QR(615) and (6) T/QR(650). (b) Fluorescence spectra after separation of highlighted bands and deconvolution results for lane 3. (c) AFM image of dual QR assembly (3). (d) Confocal imaging of dual QR+Origami assemblies in aggregates form immobilized in acrylamide gel highlighting emission from stained origami (green), QR(615) (orange), and QR(650) red.

One advantage of DNA-mediated assembly is the programmability of multiple interactions acting in concert. Built into the origami's design is the ability to mix and match the capture strands in the particular zones, affording assembly of multiple QRs simultaneously. To demonstrate this, Zone B of the substrate (see Fig. 1) was modified with a *T'*-type sequence, and a second *T*-capped QR, with emission at 650 nm (denoted as *T*-QR(650), l/w = 8.8 ± 1.4 (l = 50.1 ± 6.1 nm, w = 5.7 ± 0.4 nm) was assembled simultaneously with *U*-QR(615), producing a two color origami. The incorporation of both capture strands onto the origami was confirmed using fluorophore labeled *U* and *T* strands (data not shown, see reference). To address the issue of heterogeneity in assembly described above, the two color QR+origami conjugates were purified by gel electrophoresis (Fig. 6). For example, Figure 6 shows a typical gel of the QR+origami assembled with QR(615) alone (1), QR(650) alone (2), and both QRs (3). The band that had mobility similar to a stained origami substrate (4) was extracted, thus separating it from the excess QRs, which had greater mobility (5-6). Fluorescence measurements of the gel slice (Fig. 6b) revealed emission characteristics similar to that of the free QR for samples originating from (1) and (2), and a broad convoluted spectra for the dual assembly (3). AFM imaging (Fig. 6c) showed the presence of bi-functionalized origami, with one assembly zone showing higher features, suggesting location of the larger QR(650). Figure 4d shows confocal microscopy results for a macroscopic collection of the dual assembly conjugates immobilized in acrylamide gel. The green emission is from the origami that was stained for imaging purposes (GelSafe Green), as well as orange and red color assigned to 615 and 650 nm emission, confirming the incorporation of both rods onto the origami. Based on the steady state and confocal fluorescence results, little inter-QR Förster Resonance Energy Transfer (FRET) can be observed. This is supported by the knowledge that the QR(615) and QR(650) had comparable QY values before and after assembly, and the similar intensity contributions of the assembly spectra (see deconvolution insets of Fig. 6b (3)). This was anticipated given the large distances ($r \approx 75$ nm) between the QR on the origami, which is greater than Förster distances (r_0 = 15.9 nm, see SI). It is important to note that this lack of FRET is not a failure of the assembly itself, as the current Zone A and B assembly was designed to test and prototype conditions, particularly imaging assembly. On going work focuses on closer inter-QR distances, as well as varied orientation angles.

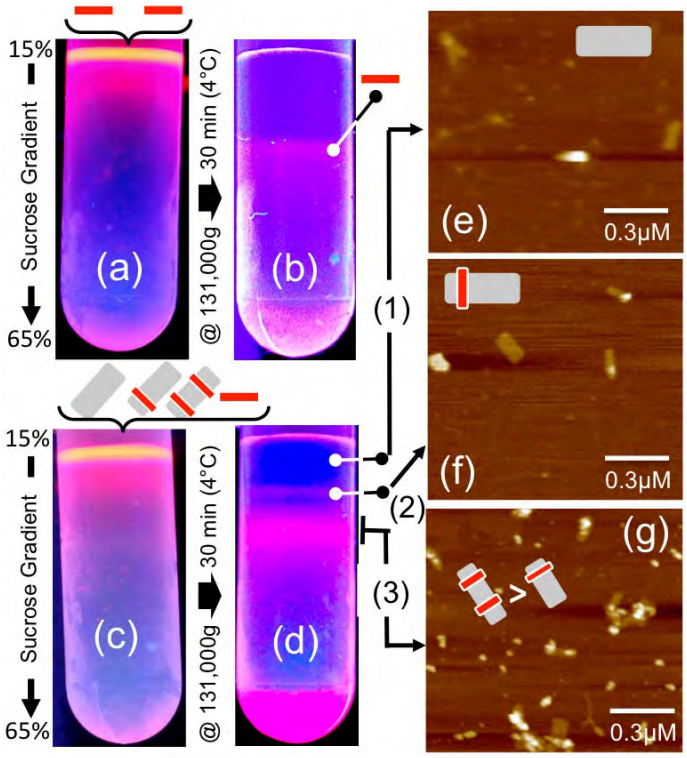

Figure 7: Representative gradient ultracentrifugation results for *U*/QR(650) (a-b), and *U*/QR(650)+origami assembly solutions (c-d) before and after centrifugation. The *U*/QR+origami assembly could be separated into three regions (1-3). AFM analysis (e-g) of the regions show unreacted origami in (1), large populations of mono-functionalized origami (2), and a broad regions with higher populations of dual-functionalized origami in the presence of free QRs (3).

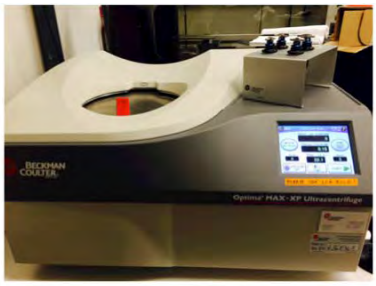

Beckman Coulter Optimax ultra-centrifuge purchased from grant.

One challenge encountered in this agarose-based separation was the loss of QY during purification. Which we attribute to the weak histidine- and DNA-capping's inability to protect at the high ionic strengths, increased temperatures, and high voltages used during long electrophoresis runs. To address this, gradient ultracentrifugation (denoted as UC) separation was explored as an alternative strategy. A Beckman Coulter UC instrument was purchased from grant and used extensively too scale up our purification capabilities (see photo to right). Recently, sucrose gradient UC has been used to purify origami structures as well as metal nanoparticle assemblies. Figure 7 shows a typical UC experiment for *U*-QRs (a-b), and crude *U*-QR(650) + origami assembly solutions (c-d) before and after centrifugation at 131,000g for 30 min at 4 ^{o}C in a 15-65 % (w/v) sucrose gradient that also contained 100 mM NaCl. As shown, the isolated *U*/QR(650) travel in a uniform band (a-b), whereas the *U*/QR+origami conjugates separate into three regions (c-d). The top region (1) was determined via AFM (e) and gel electrophoresis (not shown) to consist largely of un-reacted origami, likely mis-folds or defects that did not have incorporated capture strands. In region (2), the fluorescence color of the QRs was noticed, and AFM observed regions that consisted largely of mono-functionalized origami. The lowest band (3) was found to contain bi-functionalized (both zones consisted of *U*/QR(650)), origami and also free QRs. The UC approach had a number of advantages over gel electrophoresis, including; increased throughput (i.e. separation volumes), and preserved optical properties. One primary factor in this is the temperature controlled environment during UC, which is important since it preserves QY and also ensures against

denaturation of the DNA linkages. Future work will explore in detail the conditions necessary to improve separation of the assemblies further.

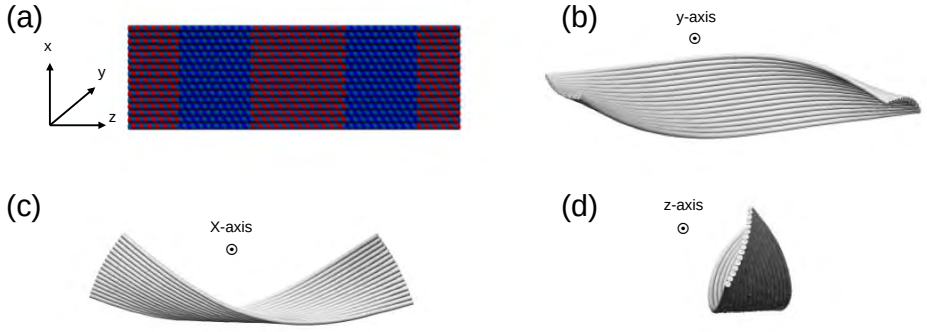

Figure 8. Images of the static origami as designed in caDNAno (a) and after CanDo modeling as viewed from the y, x, and z axes (b,c, and d, respectively). Significant bending is observed at the ends of the origami that likely displaces the capture strands from the idealized "row" anticipated in the static structure.

Table S2: Modeling Parameters for DNA Origami Mechanical Properties used in CanDo simulations.[13,14]

Property	Value
Axial Rise per base Pair	0.34 pN
Helix Diameter	2.25 nm
Crossover Spacing	10.5 bp
Axial Stiffness	1100 pN
Bending Stiffness	230 pN m^2
Torsional Stiffness	460 pN m^2
Nick Stiffness Factor	0.01

Like many chemical reactions and self-assembly systems, our final morphologies have modest yields (i.e. bi-functionalized origami). While purification methods will continue to be developed and optimized, we consider briefly the limiting factors at play in the current system. A first consideration is the QR itself, and the modest DNA surface coverage (14-17 ssDNA/QR), which considering the rod morphology, equates to footprint of ≈ 30 nm^2/ssDNA. This footprint is much larger than a typical DNA-capped gold nanoparticle system, for example, where footprints range from 6-16 nm^2/ssDNA. This, combined with the ~6 nm distance between capture strands on the origami, result in the likelihood of a lower number of QR-to-origami linkages, and subsequent decrease in cooperative binding, which in turn will result in lower hybridization energies and reduced orientation fidelity. The second reason may be the result of the assembly approach. The QR + origami assembly is carried out while both are suspended in solution, in contrast to examples that first immobilize the origami on mica, followed by nanomaterial assembly.[27] We chose our approach in hopes of scaling the yield of final product. However, additional analysis has revealed that the origami used is not an entirely rigid structure. For instance, shown in Fig. S12 are simulation results of the mechanical properties of the origami calculated using the CanDo software package (Table 2). The results reveal considerable flexibility, which in retrospect is

understandable considering the single duplex thickness (Fig. 8). In particular, the regions occupied by Zone A and Zone B are affected, and this flexibility may be limiting recognition of the QRs by both steric and osmotic effects. Uranyl acetate stained TEMs (Fig. 9a) and AFM (Fig. 9b) images both confirmed flexibility. This flexibility can be decreased in the future by altering the staple strand design in those areas, or by using a more rigid origami through a honeycomb lattice strategy to impart strength and shape control.

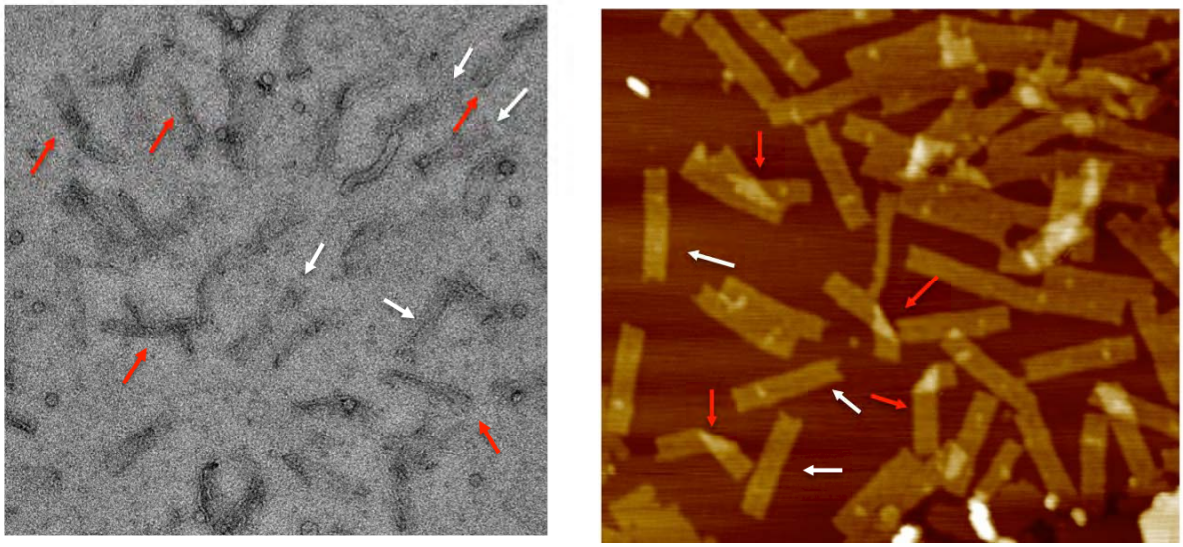

(A) (B)

Figure 9. Representative (a) 2% uranyl acetate stained TEM and (b) AFM images showing the degree of flexibility of the DNA origami. in agreement with CanDo modeling agreements. Red arrows indicate high deformed structures while white arrows show flat origami. Deposition conditions were in 12 and 100 mM Mg^{2+} concentration for TEM and AFM, respectively.

Second Generation Design: From July – Dec 2014 we continued this project by focusing on improving the structure of the DNA Origami. *We note again that the goal is not to design new and elaborated origami, but instead simply to use it as patterning tool to organize the rods.* In this second-generation system, the origami has improved surface rigidity through the adoption of a hexagonal lattice developed by Shih and coworkers. Figure 10 shows the second generation DNA origami substrate viewed from the top (A) and end (B). Modeling indicates that the second-generation structure is significantly more rigid than the single helix system we used above. The implementation of a hexagonal lattice, however, results in significantly smaller lengths (111 nm vs. 155 nm) and width (31 vs. 50 nm) compared to the first generation structure. In order to retain the different capture zones inherent to the first design, spacer regions at the ends and in between Zones A and B have been deleted (Figure 10), resulting in a 7 nm gap between the two zones. This however is especially advantageous for a generating FRET active structure, as this distance is less than half the Förster distance predicted for two freely rotating QRs (R_0 = ~16 nm). Moreover, the zones are asymmetric to accommodate a shorter and longer QR, resulting in better hybridization and orientation control.

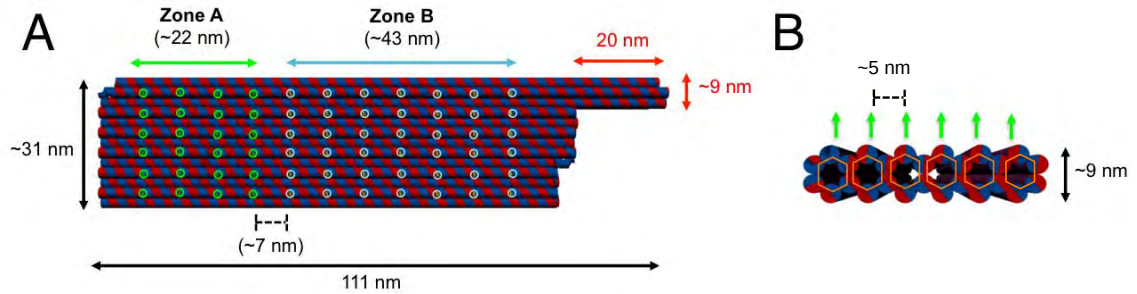

Figure 10: Schematic of the second generation DNA origami substrate for capturing quantum rods viewed from (A) the top and (B) the end of the structure. The asymmetric "finger" dimensions are indicated in red, as well as the corresponding dimensions of Zone A (green) and Zone B (blue).

In addition to the removal of a spacer region between the two capture zones, the newest design is predicted to be substantially thicker (Figure 10b) compared to the single helix structure which makes AFM quantification easier, and leads to better resolution for stain-based TEM analyses. The new design also has a morphological landmark, as shown via a asymmetric "finger" like end of the origami, which will allow for determining which zone is assembled via AFM imaging (location direction of finger, etc.). Due to the inherent length of M13mp18, the finger is only allowed to extend 20 nm from the end of the structure and is only 9 nm wide. However, this should be sufficient for AFM imaging using a ultra sharp tip with a typical radius of ~8 nm. In the hexagonal lattice, staple strands crossover the main strand every ~7 bp rather than every 10.5 bp in the Rothemund strategy. Figure 11 shows a preliminary AFM image of these second generation origami.

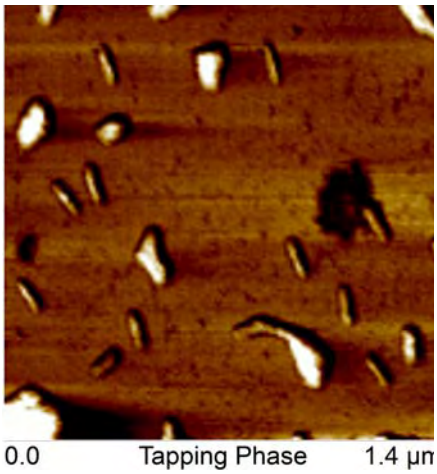

Figure 11: Preliminary AFM tapping mode image of new DNA origami structures, seen as rod like shapes.

While this provides substantial improvement in rigidity, these structures are also more difficult to fold correctly. Recent work by Shih has found that designing staple strands forming 14 straight bp with the M13mp18 scaffold strand form better structures. Our second generation structure has ~65% of staple strands which obey this design principle (Figure 8), which may be the upper limit based on where the strands must terminate to extend the ssDNA for QR capture away from the substrate. Moreover, we have updated our synthetic protocol to take advantage of lower temperature DNA folding and PEG/depletion based purification to improve yields and purity. Initial studies have shown that we can obtain dense solutions of the origami without significant amounts of excess staple strands that could interfere with subsequent assemblies. Our preliminary evidence suggests that these structures are much more sensitive to the ionic composition of the solution which we are currently optimizing for QR assembly.

Due to the grant ending, we have not yet assembled the QRs at the new origami.

The postdoctoral fellow has had to move to a different grant to maintain support in the lab. However, he is lending his expertise to a new first year graduate student who has picked up the project. She (Yeutian Chen) is an excellent student and I am confident she will be able to transfer the technology needed to continue this, or another supported QR-based assembly system. The postdoc has intentions to stay in our lab to continue this science if a new grant is awarded in the new fiscal year.

Conclusions & Prospectus

From support of this project, and from its five-year evolution, we have become the first research team to devise a way to self-assemble quantum rods into a patterned orientation on surfaces using DNA and DNA Origami. We synthesize the rods with specific aspect ratios and optical properties. The attachment of ssDNA to their interfaces was accomplished using new routes developed by us, and we transitioned towards focusing on rods in year 4-5 due to the originality and interesting challenges of that work. We also transitioned to using DNA origami over the past two years. *We make special note here, that the use of origami in our project was simply a way to pattern the rod assembly, and we do not, in this grant, intend to focus on origami design advancement.* From this project we were able to devise a new way to functionalize QR with ssDNA and to test ways to purify and collect the assembly conjugates. This project evolved out of our previous work (in years 1-3) that where we focused on assembling quantum dot clusters using DNA. Moreover, as the rods have tunable asymmetry and polarized emission, it seems logical to push the field into a new area where we focused on aligning quantum rods for the first time.

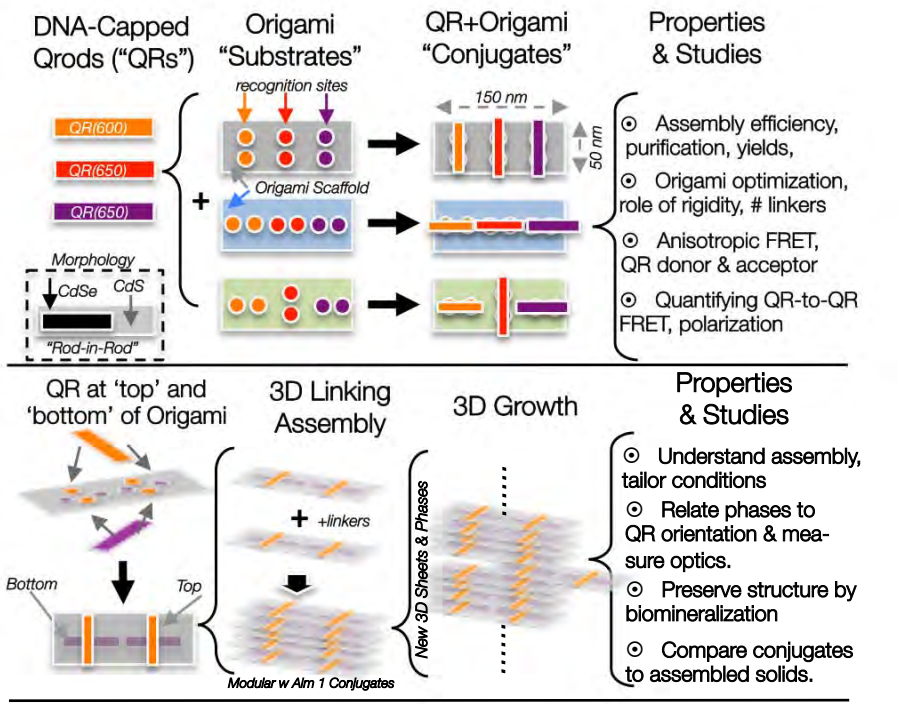

Figure 12: Scheme of future advances that can be made using this rod biomimetic assembly approach, where alignment of rods can lead to new advances in energy transfer (Top Panel), and three dimensional growth of assembled rods can lead to new phase behavior and functional biotic-abiotic metamaterials (Bottom Panel).

Figure 12 shows a schematic illustration of the near and long term future of this project, where rods with different emission colors and energies are aligned in different geometries and with different physical (and optical) overlaps (Top Panel). This would allow researchers to probe energy transfer between rods for the

first time, and also provide a new way to guide light (via energy transfer) in different directions on surfaces or solids. To achieve these goals however, would require researchers to synthesize rods with different optical and morphological properties, as well as to separate and purify the assembled conjugates (or optimize yields) in bulk manners. The bottom panel of Figure 12 shows the further self-assembly steps that can be taken using these conjugates to form 3D solids with new phase behavior and metamaterials properties. In these projects again, the purpose of using DNA origami would be for nanoscale patterning only, and the focus would not be on creating new origami science. The AFOSR support of our project has laid the groundwork for such advances.

Section 2: Understanding Bioluminescence Resonance Energy Transfer between Luciferase Enzymes and Quantum Rods (Completed)

Personnel: Lili Karam (summer RA), Kaitlin Coopersmith (unsupported RA)

Months : June-December, 2014

Publications from grant:

1. R. Alam, L.M. Karam, *T.L. Doane,* J. Zylstra, D.M. Fontaine, B.R. Branchini, **M.M. Maye*** *"Near infrared bioluminescence resonance energy transfer from firefly luciferase-quantum dot bionanoconjugates"* ***Nanotechnology*** **2014**, 25, 495606.

Publications from grant in preparation:

2. R. Alam, L.M. Karam, T. Doane, D. Ablamsky, B. Branchini, M.M. Maye* *"Investigating the Origins of BRET efficiency in Luciferase modified Quantum Rod Nanosystems"* **2015** (In preparation)

Presentations:

- **M.M.Maye** *"Designing Nanomaterial Architectures for Applications in Self-Assembly, Drug-Delivery, and Energy Transfer"* ACS Susquehanna Valley Section Lecture, March 12, 2014, Susquehanna Univ.

Summary: In this section we discuss the continuing development of the bioluminescence energy transfer project and collaboration with Prof. Bruce Branchini at Connecticut College. In year 5 of this grant, we spent about half of the year focused on analyzing and publishing our results from the previous year, and focused experimentally on understanding and optimizing the energy transfer stability over time. In addition, Prof. Branchini supplied us with a new Ppy mutant (histagged PpyGR7), that has brighter bioluminescence with the $BtLH_2$ substrate he prepared in year four. During this time, one summer RA was supported on the project, and she worked on the project as a TA in the fall semester. *The primary goals* of this section are to; (*i*) study biotic-abiotic energy transfer using bioluminescence resonance energy transfer (BRET) (***goals amended in year 2)***, *and to (i)* investigate the BRET efficiency between firefly Ppy enzymes and quantum rods (***goals achieved in year 3-4***), (*ii*) to understand and improve the long term stability of the systems (***goals achieved this year***); and to (iii) optimize the brightness of the system (***milestone slipped in present year***).

Results & Discussion: As discussed in last years report, we used our self-assembly technology and quantum dot (QD) synthesis to prepare BRET nanoconjugates that emit in the near infrared light (nIR) region, which has many potential uses, including night time sensing and signaling, as well as imaging and bio imaging. Figure 13 shows a schematic for review.

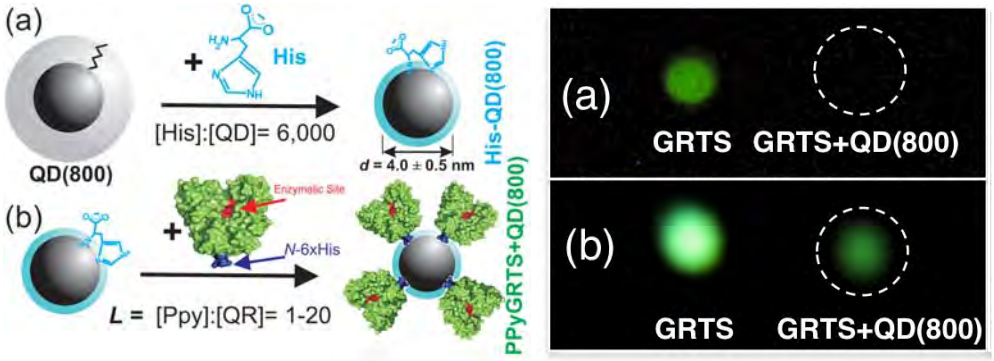

Figure 13. LEFT PANEL: (a-b) An idealized schematic of the alkyl-capped QD(800) QDs that were phase transferred by ligand exchange with histidine (His), which rendered the QD(800)s hydrophilic and colloidially stable (a). Next the QDs are incubated with 6xHis tagged PPyGRTS at increasing loading ratios, *L* = [PPy]:[QD(800)], between 0.5 - 10 (b). RIGHT PANEL: (a) Photograph comparing the bioluminescence of PPyGRTS (left), and PPyGRTS+QD800 BRET (right) taken with standard digital camera (a), and a digital camera attached to night vision goggles (b). Note that the green color in b is an artifact of imaging, and not the true color of the systems.

After making some advances in our ability to quantify PpyGRTS loading at the QD(800) QDs, we were able to successfully publish the results in *Nanotechnology* this year. Since many of the data or analysis were reported in year 3 & 4, I focus here only on the new results.

We focused on quantifying the PpyGRTS loading/conjugation via non-traditional method, that of thermal gravimetric analysis (TGA). Here, mass loss during heating/burning of the PpyGRTS-QD(800) is directly related to the lightweight His monolayer, and the heavier PPyGRTS (MW ≈ 60 kDa). Figure 14a shows a representative TGA profile for the QD(800) before (i), and after (ii) phase transfer, where a mass loss of 51% and 25% was measured, respectively. These results provide conformation of monolayer exchange and subsequent phase transfer, since the His has much lower MW compared to typical hydrophobic capping ligands like TOPO, etc. For the PPyGRTS+QD(800) conjugates, a mass loss increase was observed as a function of increased *L*. Specifically, as *L* increased from 11-43, a successive increase from 66 to 88% was observed (iii-v), indicating increased weight loss due to additional proteins residing on each QD. Next, the conjugates were first studied in detail using Fourier transform infrared spectroscopy (FTIR) (Figure 14b-c). Compared to the His-QD(800) (i), the PpyGRTS+QD(800) conjugates show sharp vibrations at ≈1627, 1551 cm^{-1} for *L* = [PpyGRTS]:[QD(800)] = 10 (ii), which are characteristics of amide-I and amide-II modes originating from the protein. Amide-III modes are also present at ≈1290 cm^{-1}. While the amide-I modes are due to C=O stretching, amide-II and III are attributed to CN stretch and NH bend within the protein. There are also sharp vibrations at 3177-3184 cm^{-1}, indicating the presence of amide-A and B modes, which arise from NH stretching.

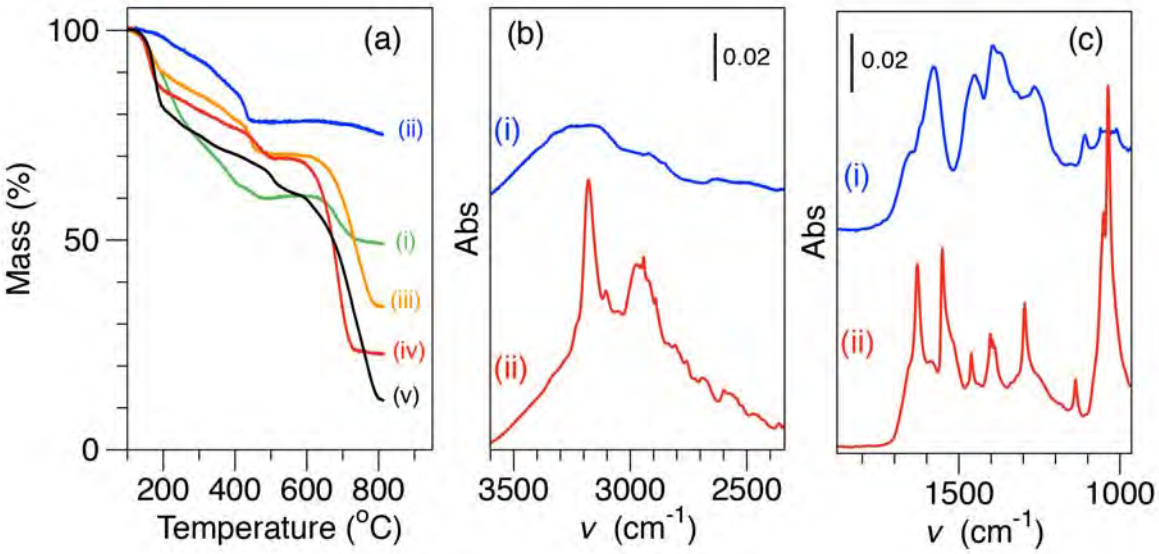

Figure 14. (a) TGA results characterizing the original hydrophobic QD(800) (i), the His-QD(800) after phase transfer and purification (ii), and the PPyGRTS-QD(800) conjugates at *L* = 11 (iii), 22 (iv), 43 (v). (b-c) FTIR characterizing the low and high-energy vibration regions for His-QD(800) (i) and conjugates at *L* = 10 (ii).

The other main focus of this project, studied over the summer and some of the fall '14, was to improve the long-term stability of the PpyGRTS-QR conjugates. Previously, BRET was studied within a few hours of conjugation, however within a few days, the conjugates were found to decay so that BRET efficiency (BRET Ratios, BR) decreased rapidly (Fig. 15a). We were not sure the source of this decay, and there were a few possibilities; (i) the PpyGRTS could be decaying on its own over time, (ii) the QR could be looking quantum yield over time (iii), or the conjugation itself was changing over time, possibly leading to denaturing of the PpyGRTS at the QD interface (iV). Over a long study simplified in Fig. 12, we found that the loss of BR was due to two factors. First, the Histidine-capped QRs decayed over time

via flocculation, which could not be redispersed. And in addition, control experiments showed that the PPyGRTS was indeed denaturing over time when bound to the interface.

To address this, we assayed a number of different surface capping ligands for the QR that provided stability, while at the same time, did not block PpyGRTS adsorption. After a number of trials we decided on using glutathione (GSH). Figure 12 shows the results of a typical weeklong stability study. The PPyGRTS itself was stable over the time period (Fig. 15d), and the PpyGRTS functionalized QR (with GSH capping) showed little to no loss in QY over the time course (Fig. 15 c), which demonstrates the optical and hydrodynamic stability (no flocculation) of the conjugate as well as the two optical sources. Second, the BRET BR values measured over this study showed only fluctuations (+/- ≈ 20%) (Fig. 15b), which is significantly better than the PPyGRTS-QR with His-capping (Fig. 15a). The GSH molecule has been used previously in the gold nanoparticle field, and is known to be zwitterionic at the pHs used in our study, and thus moving forward, we will need to start to use GSH or similar molecules to improve stability of the systems.

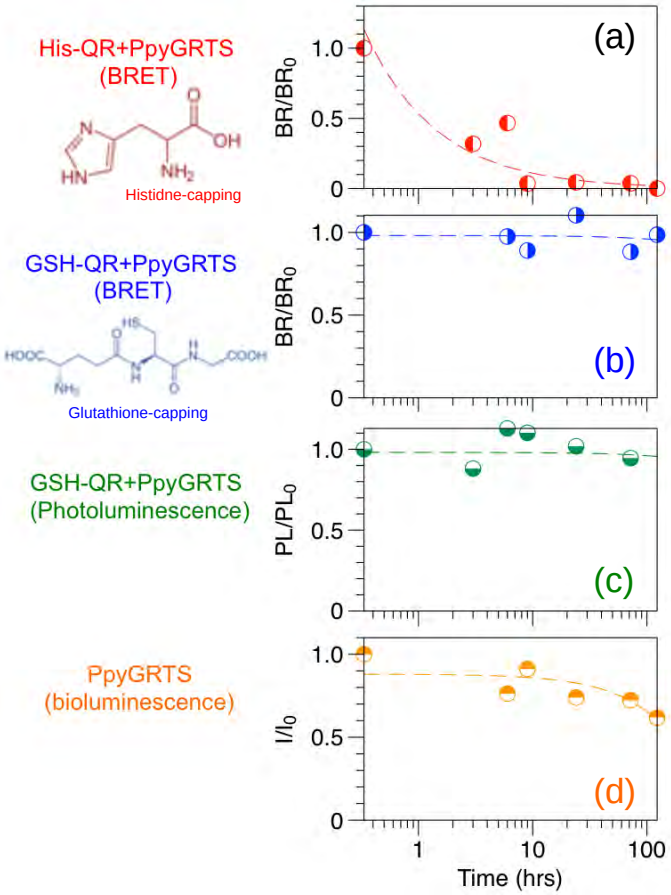

Figure 15: Stability plots corresponding to traditional His-QR+PpyGRTS Bret Ratio (BR) (a), BR from GSH-capped QR+PpyGRTS (b), and controls characterizing fluorescence stability of the GSH-QR+PpyGRTS (not under BRET) (c), and PpyGRTS bioluminescence over similar time periods. Results indicate significant improvement of BR stability in new GSH-capped conjugate in b.

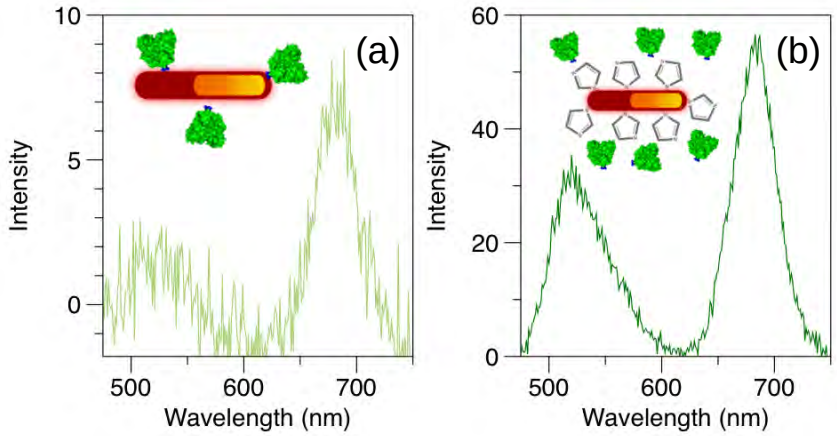

Figure 16: Preliminary BRET experiment probing non-radiative (a), and radiative (b) BRET. A typical BRET spectra is shown in (a) for a PpyGRTS-QR system at L = 10. High BRET ratios (BR ≈ 2.5) are shown, however the systems typically has low brightness. When the same conjugate is injected with a high concentration of imidazole or GSH a brighter optical response is observed (see intensity values on y-axis), due to the PPyGRTS undergoing a typical bioluminescence, and the QR absorbing the excitation (inner filter effect).

This year we also tested the relationship between non-radiative and radiative BRET in our systems. As we have reported previously, at low *L*-values where the QR surface is unsaturated with PPyGRTS, high BR are observed, but also low general intensity (i.e., brightness). However at higher *L*, the BR decreases along with a significant increase in overall brightness. To understand this phenomena better, a number of experiments and studies were performed. One such study is shown in Figure 13. Figure 13a shows a typical BRET signal, where the emission at ~690 nm is coming solely from the accepted energy of the excited state of PpyGRTS+LH_2. During BRET emission, we injected into the solution an excess of imidazole, which both binds to the QR interface, but also saturates the PPyGTS histagged N-terminus, thus liberating it from the QR. As a result of liberation, the PPyGRTS starts to bioluminescence normally, as observed by the increase emission at 550 nm. Interestingly, due to an inner filter effect, the QR can absorb this emission and then emit itself, thus showing the signal at 690 nm. It is not clear at this moment why the BR values are only slightly different, and this may be a coincidence of the QR concentration in solution (additional concentration dependence studies proved this). Nonetheless, these experiments were very important in our understanding of the energy transfer mechanism of our system. These studies conclude the data that is needed to publish a large report on BRET using QR interfaces. However in future work, a more sophisticated thorough study is needed where PPyGRTS-to-QR distances can be controlled and tailored, and the resulting BR can be then modeled as versus a number of non-radiative or radiative models.

Conclusions & Prospectus

The AFOSR's support of this project has allowed us to become one of the most creative research groups studying biomimetic energy transfer, and the combination of two AFOSR researchers (Prof. Branchini and ourselves) has produced a new synergy in the field. Our 2012 *Nano Letters* paper has been cited 21 times. Compared to the other primary researcher in this BRET conjugates area (Rao, Stanford Medical School) who focuses on using BRET-conjugates for medical imaging, we focused on understanding the fundamentals of the energy transfer, and while doing so, created the most efficient energy transfer system using bioluminescence. Thus, our projects have more of an industrial application, relating to lighting, signaling and sensing. These areas of research are where we can make a significant novel contribution.

That being said, this last year of the grant was slower on the new discoveries front for this project, and I am disappointed with the progress we have made. I transitioned the project between a number of grad

students who, due to a range of personal problems and other commitments during the semesters, where not particularly productive. We are still working on this issue, and trying to recruit new students (or train existing good students) on the system. Scientifically, moving forward, our BRET nanosystem approach has two critical hurdles it needs to overcome, and one potentially transformative application.

These hurdles are; (*i*) understanding the exact binding mechanism and location of the PpyGRTS (and it's mutants) at the quantum rod interface, and (2) increasing the overall brightness of the system by using *both* more efficient PpyGRTS donors (brightness), and nanomaterials (quantum yield). In the first goal, a series of cryo-TEM, in-situ AFM, and single molecule spectroscopy works are needed. Over the half-year we have begun to address these limitations in our studies. First, I worked to start a strong collaboration with a cryo-TEM expert who has an instrument capable of the resolutions and digital reconstructions needed (Prof. Stephan Wilkens, SUNY-Upstate Medical School). Myself and another student are now trained on the instrument, and have performed a series of initial negative staining experiments with him. The cryo-work is now planned, and will be a hybrid of both traditional imaging and protein structure reconstruction. AFM studies are now possible in our lab using the AFM purchased from the grant (section 1), and using ultra sharp AFM tips will allow us to probe individual QRs and protein location. Single molecule studies were attempted in year 2-3, and the conjugates were found to be not bright enough to be observed at the single molecule level. We have not made progress in this area this year, but I strongly believe that these experiments are possible, but another limitation is the fundamentals of bioluminescence, and its un-correlated energy transfer to the quantum rods (no time correlation from input laser light to photon emission, for instance). This is in contrast to traditional single molecule studies. However, advances in detector sensitivity (in the nIR) of our collaborators instruments may resolve the sensitivity issue, and it thus may be close for us to determine brightness at the single rod level over the next year.

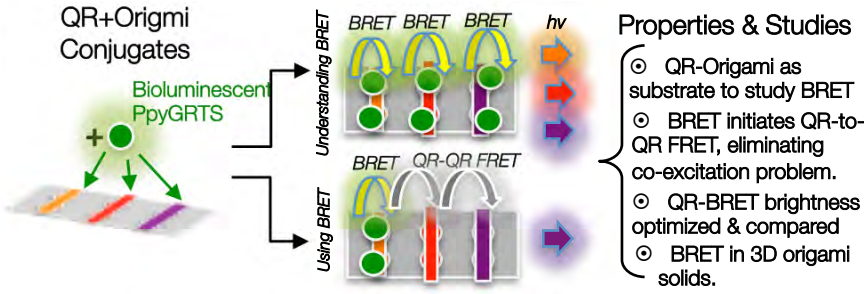

Figure 17: Scheme of future BRET nanosystem studies that can be performed in combination with other proposed projects.

To further improve the overall brightness of the system, it may be required to study other nanomaterials as acceptors. For instance, very recently (winter 2015) researchers synthesized so-called cesium-lead-halide perovskite nanoparticles for the first time, which have size and composition tunable optoelectronic properties comparable (and possibly better than) qdots like CdSe/ZnS (see Potesescu, et. al. *Nano Letters* **2015**, ASAP, DOI: 10.1021/nl5048779). We have successfully prepared these materials in our lab, and their quantum yields are consistently >70% (see image below). The ability for materials like these too accept energy, especially from a bioluminescent source is unknown, and a frontier in the biotic-abiotic field.

In addition to exploring new materials, I believe the main application in the future for BRET nanosystems will be the excitation of bulk assembled "solids" or single particle "flares" that induce energy transfer.

Today, almost all non-radiative energy transfer systems utilize external light as an excitation source. In nanomaterials, this excitation can often co-excite all of the materials. This "co-excitation" has long been

trumpeted for quantum dots in bio imaging since a single laser can excite many probes. But in actuality, this is a significant limitation in the field of self-assembly and metamaterials. As the field's assembled nanostructures have increased in complexity and sophistication (crystals, clusters, *etc.*), our ability to excite specific components has not. There is no way for example, to excite only a gold nanoparticle or a particular qdot with a laser without exciting the entire system. Thus, in the future, highly optimized bioluminescent materials (and their bio-nano interfaces) will be used to selectively excite nanoparticles, thus removing the need to external light sources, while at the same time selectively turning on individual components at will.

Photo of perovskite-dot emission, tuned by composition

We hope to pioneer this area of research, and Figure 17 shows a few possibilities for this project in the future. As a starting point, consider our QR assembly systems from section 1, where BRET can be used to initiate signaling and energy transfer on only those rods where it is attached. The light could be used as a sensor to detect multiple targets, or to guide/model energy transfer through a solid or cluster. This also would allow for us to overcome the challenges of co-excitation, and to introduce new biotic-abiotic energy transfer phenomena. The AFOSR support of our project has laid the groundwork for such advances in the future.

Section 3: Tuning DNA-mediated Nanoparticle Interactions using Smart Thermosensitive and pH Sensitive co-Polymers for Assembly and Crystallization (COMPLETED)

Personnel: Jay Tinklepaugh (unsupported RA (supported via NSF IGERT Training Grant), Kristen Hanmer (RA + partial summer support, graduated with PhD in July 2014), Simon Pun (Undergraduate), Olivia Sheppard (High-School).

Months : January-December, 2014

Publications that cite grant:

1. C. M. Alexander, K. L. Hamner, **M.M. Maye***, J.D. Dabrowiak* "*Multifunctional DNA-Gold Nanoparticles for Targeted Doxorubicin Delivery*" *Bioconjugate Chem.* 2014, 25, 1261-1271.

Primary Publications from grant, in Preparation (Data Collection Complete):

2. K.L. Hamner, S. Pun, D. Smilgies, J. Tinklepaugh, M.M. Maye* *"Small Angle X-ray Scattering Investigation of 3D Nanoparticle Assemblies with DNA and Thermosensitive co-Polymer Linkages"* ***Journal of Physical Chemistry Letters*** **2015** *(*In submission)
3. J. Tinklepaugh, S. Pun, O. Sheppard, M.M. Maye* *"pH Sensitive Smart Nanoparticles"* **2015** (in preparation).

Presentations:

- **M.M. Maye**, K. Hamner, J. Tinklepaugh, S. Pun, D. Smilgies, "Using Smart Polymers to Regulate DNA-Mediated Nanoparticle Assembly, Crystal Formation, and Interparticle Spatial Properties" MRS Fall Meeting, Boston Mass. 2014
- **K. Hamner** "Using Temperature-Sensitive Smart Polymers to Regulate DNA-mediated Nano Assembly" PhD Defense, July 25, 2014.
- **J. Tinklepaugh**, M.M. Maye, "Functionalization of Nanoparticles with Smart Polymers for Controllable Self-Assembling Systems" Syracuse Biomaterials Institute Stevenson Lecture Poster Session, October 2014

Summary: In this section we describe the work performed this year related to introducing "smart" components into bio-inspired nanoparticle self-assembly. We focused on understanding and publishing the results from late last year, and to extend our approach to using pH sensitive co-polymers as well as elastin-like polypeptides that have smart characteristics. Of particular importance this year was the finding that the pH sensitive co-polymers can be used as a way to tailor the charge, and magnitude of charge of nanoparticles. In this report we briefly describe the properties observed, demonstrate pH smart behavior of nanoparticles, and show a new paradigm in electrostatic self-assembly. *The primary goals* of this section are to; (*i*) explore the ability to self-assembly nanoparticles into 3D assemblies with long range order (***goals accomplished in year 3***), (*ii*) to tailor interparticle interactions by changing DNA structure, types, or by addition of new materials like smart polymers (***goals accomplished in year 4 and this year, on-going***), and (iii) to study the assembly phase behavior via SAXS ***(goals accomplished in year 4, on-going)***.

Results and Discussion: Last year's report described our recent progress in the preparation of low critical solution temperature (LCST) smart polymers with compositions of pNIPAAm-*co*-pAAm copolymer that were attached to gold nanoparticles. Following a literature approach, we used a disulfide initiator to graft the polymer to the gold surface that also possessed a quantity of ssDNA (see last years report, or references above). Depending on the temperature and the polymers critical temperature (Tc), the polymer is in an extended hydrophilic state at T < Tc, or a hydrophobic coiled/condensed state at T > Tc.

This year, we extended this approach to create a number of pH sensitive co-polymers and further extended our approach to using elastin like polypeptides. In our report last year, we showed that we have developed a number of new "smart" bio-inspired nanoparticle assembly routes that included temperature sensitivity. This year, we made a very cost-effective transition to incorporating new acrylamide monomers into the polymers that had pH sensitivity due to different protonation-deprotonation (*i.e.* pKa) profiles. Figure 18 shows two model polymers we have synthesized, which use acrylic acid (AAm) and 4-vinylpyridene (4VP) monomers, which produce negatively charged pNIPAAm-*co*-pAAm-co-pAAc

(Fig. 18 top) and positively charged pNIPAAm-*co*-pAAm-*co*-p4VP (Fig. 18 bottom), respectively. When attached to gold nanoparticle surfaces, the nanoparticles largely adopt the properties and charges of the co-polymers, namely; pH sensitivity, different charges (positive or negative) and magnitudes of those charge, as well as new thermal sensitivity and profiles. This year for simplicity, the molar ratios of monomers used were [NIPAAm]:[AAm]:[X]=80:10:10, where X = AAm or 4VP were held constant, but could be varied in the future to further manipulate properties. We briefly describe this work here.

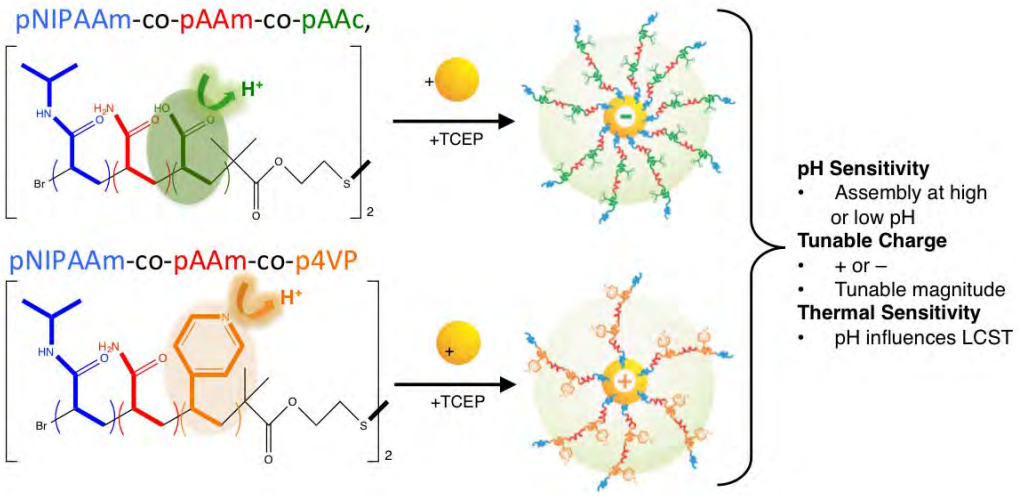

Figure 18: A schematic of the X pNIPAAm-co-pAAm-co-pAAc (top) and pNIPAAm-co-pAAm-co-p4VP (bottom) smart co-polymers, which have varied pH tenability due to the pKa profile of the AAc and 4VP groups. Surface attachment to the nanoparticles takes advantage of a disulfide bond at the center of the polymer, resulting in nanoparticles with different thermal, pH, and charge profiles, each of which can be used to tailor self-assembly.

After synthesis and purification (not shown here), the polymer's structure and composition was confirmed via ^{1}HNMR, which allowed us to estimate the concentrations of the desired functional groups in the final product. Figure 19 a representative NMR spectrum for pNIPAAm-*co*-pAAm-*co*-p4VP. The polymers molecular weight is being determined by collaborators at UMass-Amherst's MRSEC facility.

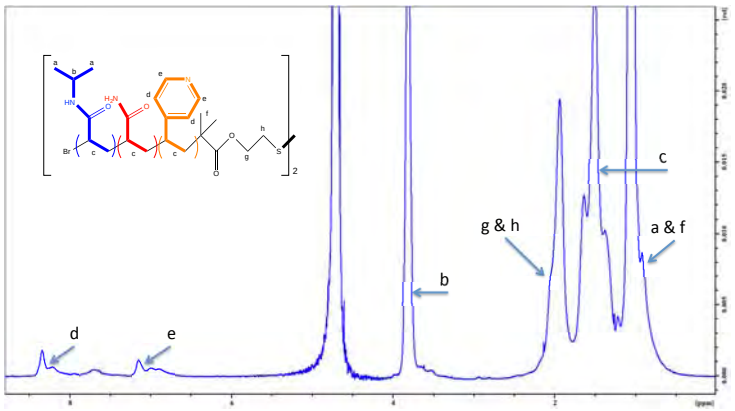

Figure 19: A schematic of copolymer pNIPAAm-*co*-pAAm-*co*-p4VP and a representative NMR spectrum. Proton locations are labeled in the schematic and corresponding peaks in the spectrum are annotated accordingly.

The pH tunability of the polymers were studied in a number of ways, include zeta-potential analysis that determines polymer charge and hydrodynamic radius (r_h) as a function of pH. Figure 20 shows a representative zeta-analysis plot for pNIPAAm-*co*-pAAm-*co*-pAAc (a), and pNIPAAm-*co*-pAAm-*co*-p4VP (b), which show negative and positive overall charges due to the protonation states of the AAc and 4VP moieties. These values can be further tuned to neutral values by change pH.

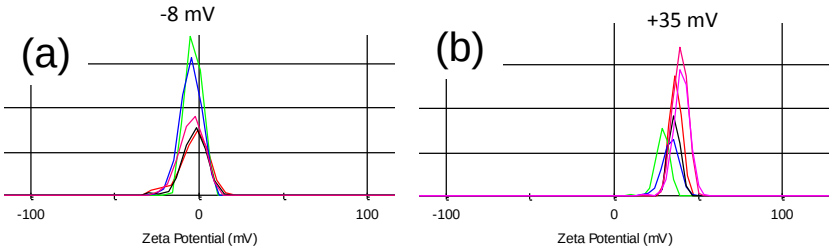

Figure 20: Representative Zeta-Potential results characterizing the charge of pNIPAAm-*co*-pAAm-*co*-pAAc (a), and pNIPAAm-*co*-pAAm-*co*-p4VP (b), revealing the negative and positive charges of the native polymers (pH = 7.0).

To determine the effect of pH on polymer critical temperature, thermal profiles of the polymers in solution were studied, and the pNIPAAm-*co*-pAAm-*co*-p4VP response is shown in Figure 21. Figure 21a shows the change in LCST Tc values across the pH scale. A decrease in Tc from 48 to 42 ^{o}C can be observed from pH 4-7, however after this, a shift to higher Tc was observed. We determined this trend was due to differences in ionic strengths used to achieve pH, and Figure 21b shows a similar pH study at constant ionic strengths. In these studies, a clear trend towards decreased Tc at increased pH is observed, due to an increasing charge of the polymer. Interestingly, these ionic strength effects were important towards understanding the polymers near a DNA interface, and many studies like these for our previous polymers were studied, which is helping us understand properties in normal buffers that DNA assembly takes place in (*i.e.* 50-300 mM NaCl), and to explain the phenomena observed in our SAXS studies.

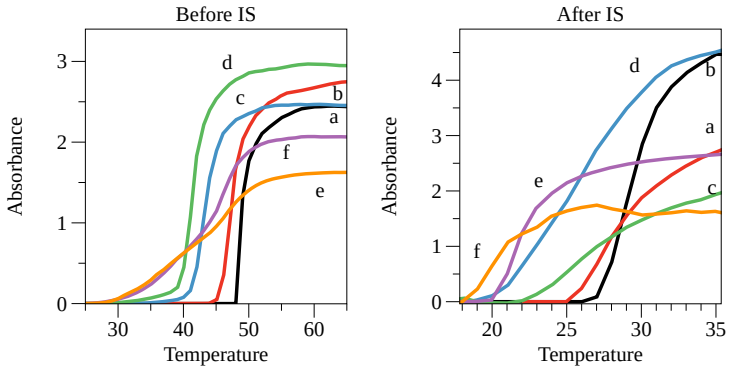

(a) (b)

Figure 21: (a) The LCST transitions for pNIPAAm-*co*-pAAm-*co*-p4VP at pH = 4(a), 5 (b), 6 (c), 7 (d), 9 (e), and 12 (f). (b) Representative polymer melts from 25-65 ^{o}C under varying pH conditions under identical ionic strength conditions. pH increases from a to f, (a) 4 (b) 5 (c) 6 (d) 7 (e) 9 (f) 12.

We next used the internal disulphide moiety in each copolymer to graft it to AuNPs (Fig. 22). To initiate the binding of polymer to AuNP the disulphide linkage was first reduced to its thiol by TCEP at high molar excess for 30min at room temperature resulting in two chains. Then polymers were added to 1mL of AuNPs in 12.5 molar excess and left to anneal overnight. Excess polymer was removed via

centrifugation and the modified nanoparticles were characterized by FTIR, TGA, and DLS (data not shown here).

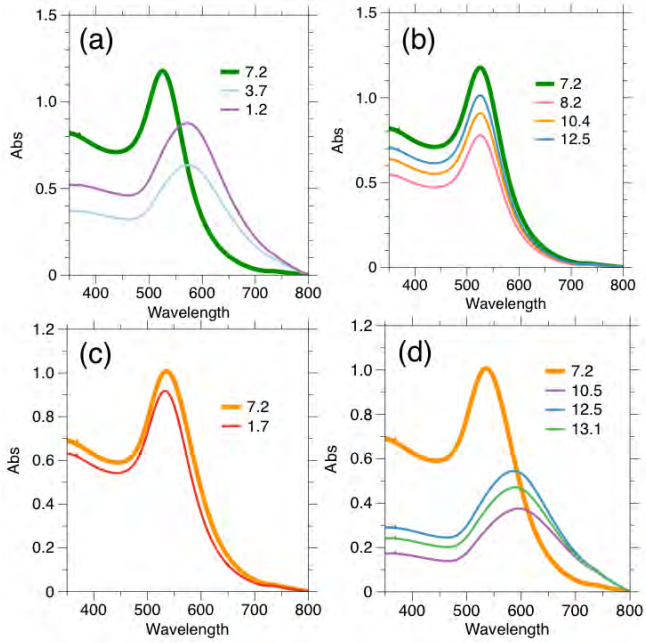

Figure 22: SPR monitoring of pH response for pNIPAAm-co-pAAm-co-pAAc (a-b), and pNIPAAm-co-pAAm-co-p4VP (c-d) capped nanoparticles, at low (a,c) and high (b,d) pH values (100 mM ionic strength).

Figure 22 shows a set of UV-vis results that the surface plasmon resonance (SPR) of the AuNPs to observe pH sensitivity. For the pNIPAAm-*co*-pAAm-*co*-pAAc capped NPs (Fig. 22 a-b), the SPR red-shifts considerably at pH < 4 (a), whereas at pH > 7 (b), only shows a decrease in absorbance values and no λ-shift. This decrease in absorbance was due to a dilution affect from adding additional buffer. In contrast, the pNIPAAm-*co*-pAAm-*co*-p4VP capped NPs show little SPR shift at low pH (c), but significant red shift at pH > 7 (d). Figure 23 summarizes these trends. While more precise control the number of pH points is needed, these titration-like assembly plots show the contrary properties of these two smart nanoparticles.

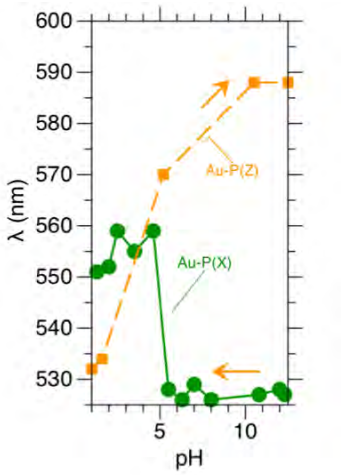

Figure 23: Summary of pH response pNIPAAm-co-pAAm-co-pAAc (green), and pNIPAAm-co-pAAm-co-p4VP (orange) capped nanoparticles. A shift in SPR (λ) is indicative of gold nanoparticle self-assembly or aggregation.

One very interesting aspect of this polymer-functionalized system is that the charges and magnitudes of the charges can be fine tuned by pH. Thus, this may open up new ways to explore electrostatic assembly of nanoparticles. For instance, mixing solutions of pNIPAAm-*co*-pAAm-*co*-pAAc and pNIPAAm-*co*-pAAm-*co*-p4VP capped nanoparticles will lead to assemblies whose long range order, crystal type, or morphology can be tuned by pH. We recently tested this, and the results are shown in Figure 24. The SPR response is very different to the typical pH-only response (Fig. 22). For example, Figure 24b show the final SPR after assembly at pH = 55, 6.0, 8.0, and >10. Little assembly is observed at the lower pHs, however a significant SPR shift is observed at the higher pH, where pH > 10 in particular show a broad two-band structure. A response like this is often indicative of forming an ordered assembly, where ordering means both interparticle distances as well as overall morphology (spheres, etc.). TEM analysis of these assemblies is ongoing, and future experiments with SAXS are planned to understand the ordering of the particles. The shift in assembly at high pH is likely

the result of the charge balances, where there is a strong positive charge in 4VP and a more neutral charge in AAm. We are currently investigating this phenomenon in detail.

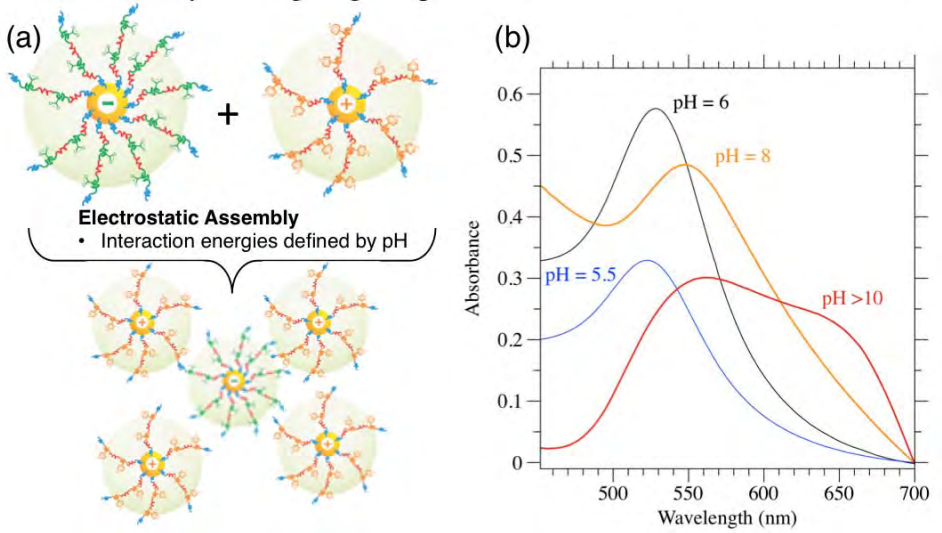

Figure 24. (a) Schematic of the electrostatic assembly driven by pH changes at the smart polymers. (b). UV-vis results for the final state of assembly at pH = 5.5, 6.0, 8.0, and >10. (T = 25 ^{o}C, 100mM NaCl)

One of the interesting next steps in our approach is to use bio macromolecules like oligonucleotides and polypeptides that can be prepared with analogous smart behavior, such as like pH or thermal-sensitivity.

To test this, we employed two commercially available polypeptides that have elastin like properties, MESLLP-$[VPGVGVPGVGVPGEGVPGVGVPGVG]_{15}$-V (denoted as ELASTIN1) and MESLLP-$(VPGVG\text{-}VPGVG\text{-}VPGEG\text{-}VPGVG\text{-}VPGVG)_{10}(VPAVG)_{40}(VPGVG\text{-}VPGVG\text{-}VPGEG\text{-}VPGVG\text{-}VPGVG)_{10}$V (Denoted as ELASTIN**2**). While these polypeptides are not perfect for the long term, each has varied ~VPG~ units, which are known to induce LCST behavior and flexibility in elastin, and also they have the Methionine (M) unit at the N-Terminus whose thioether linkage can be used for attachment to gold nanoparticles.

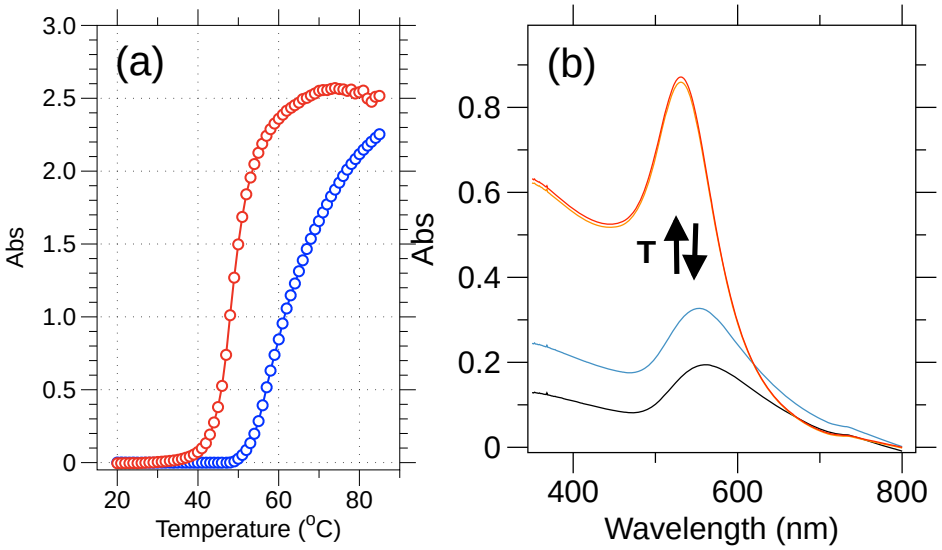

Figure 23: (a) The LCST profiles for elastin like peptides ELASTIN**1** (red) and ELASTIN**2** (blue). (b) The SPR change for ELASTIN1-capped gold nanoparticles at T<Tc (red,orange), and T>TC (blue, black). Results show that elastin like peptides can be used analogously to the smart co-polymers to drive temperature (or pH) sensitive assembly.

Figure 23a characterizes the LCST profile for the ELASTIN**1** and ELASTIN**2** polypeptides, which have Tc = 47 and 63 ^{o}C. Trials functionalizing ELASTIN**1** and ELASTIN**2** with gold nanoparticles were performed, with only ELASTIN**1** showing success, which we attribute to its shorter polypeptide length. Figure 23 b shows the SPR response change of ELASTIN**1**-capped AuNPs at T < Tc and T > Tc. As can be observed from the plot, assembly occurs in the nanosystem as indicated by the SPR decrease and red-shift/broadening. When comparing this response to our previous studies reported last year, we observe a more rapid aggregation/assembly at Tc, which may be due to the length of the polypeptide, as well as additional coordination between the peptides and the nanoparticle surface.

These results are extremely interesting, because polypeptides like these can be synthesized or purchased with more control over composition and molecular weight than polymers, opening up for more systematic control over properties in the future. Moreover, other polypeptides with pH tunability, or structural rigidity may also be incorporated into this design, paving the way for a more true-biomimetic like response. Interesting and important studies using nanoparticles like these, such as making hydrogels of these nanoparticle networks, and study of nanoparticle transport in the gels, as well as rheological changes would be a first of their kind. Moreover, a completely new angle for these nanosystems would be to more purposely prepare a hydrogel-capped nanoparticle system, which would have a very novel combination of "soft" and "hard" biomimetic interface that would lead to discoveries in a number of areas of research as well as in biomaterials like applications.

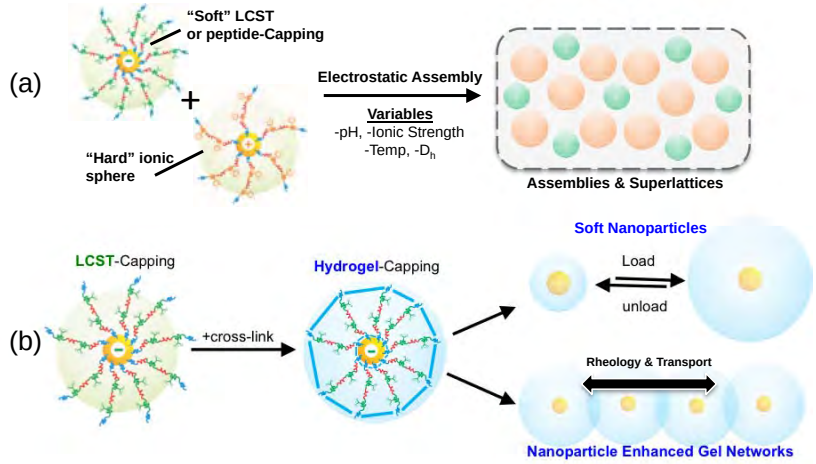

Figure 24: Scheme of future systems that explore the unknown characteristics of the LCST-nanoparticle systems. (a) The LCST- or elastin-capped nanoparticles will have a unique combination of both soft and hard interactions during electrostatic assembly, leading to new assembly and phase behavior. (b) The nanoparticles can serve as starting points to create hydrogel-capped nanoparticles for the first time, which may have unique loading-unloading (swelling / de-swelling) characteristics, as well as unique rheology and transport properties in bulk hydrogels.

Conclusions & Prospectus

Over the previous two years we used LCST polymers to regulate the way that DNA interacts with nanoparticle interfaces, and also used the phase changes as a "hydrodynamic switch" in DNA-mediated self-assembly. This year, we focused primarily on the LCST polymer and making it pH sensitive. While not an original of the project, this year's pH-response studies were critical as we make a transition from using amphiphilic co-polymers to biomaterials with similar properties. This year's work was very cost effective, and the only true charges to the grant were for cheap polymer monomers, as additional student support was from a NSF IGERT grant that focuses on "soft interfaces". However, the new discoveries that showed we could use elastin like polypeptides to do similar self-assembly open the doors for a number of novel projects in the future. Scheme 24 shows some of these possibilities.

(a) Using the pH sensitive co-polymers or polypeptides, the charges and magnitudes of those charges can drive novel electrostatic assembly of nanoparticles into organized superlattices. Here the nano-interface will have both a “hard” attractive ionic component, and a “soft” repulsive polymer component, which may lead to new assembly and phase behaviour. Moving forward, the LCST polymers would be fully substituted with the elastin-like polypeptides, which can be used as models or staring points for other stimuli responsive or structurally relevant polypeptides to control optical and strength properties.

(b) Focus should be paid to research on using the LCST polymers to purposely grow/synthesize a “hydrogel” shell around each nanoparticle (which would require some new grafting chemistry and polymer cross-linking). These hydrogel nanoparticles can then be used to model transport in bulk hydrogels, or used as the main material or a cross-linker for hydrogels, which may lead to novel rheology properties. These hydrogel-capped nanoparticles would then be transferrable to the considerable hydrogel-based biotechnology industry, and contribute to fields related to wound healing, self-healing, biomaterials, drugs, and treatments.

Appendix 1. Origami Design and Components.

Origami Left

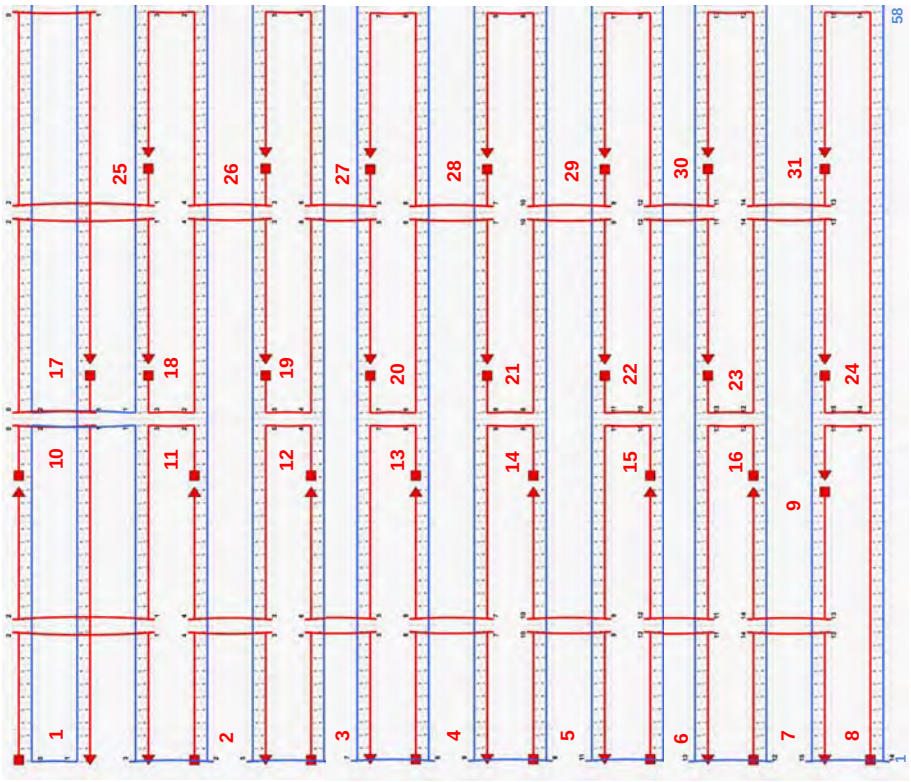

Capture Zone A

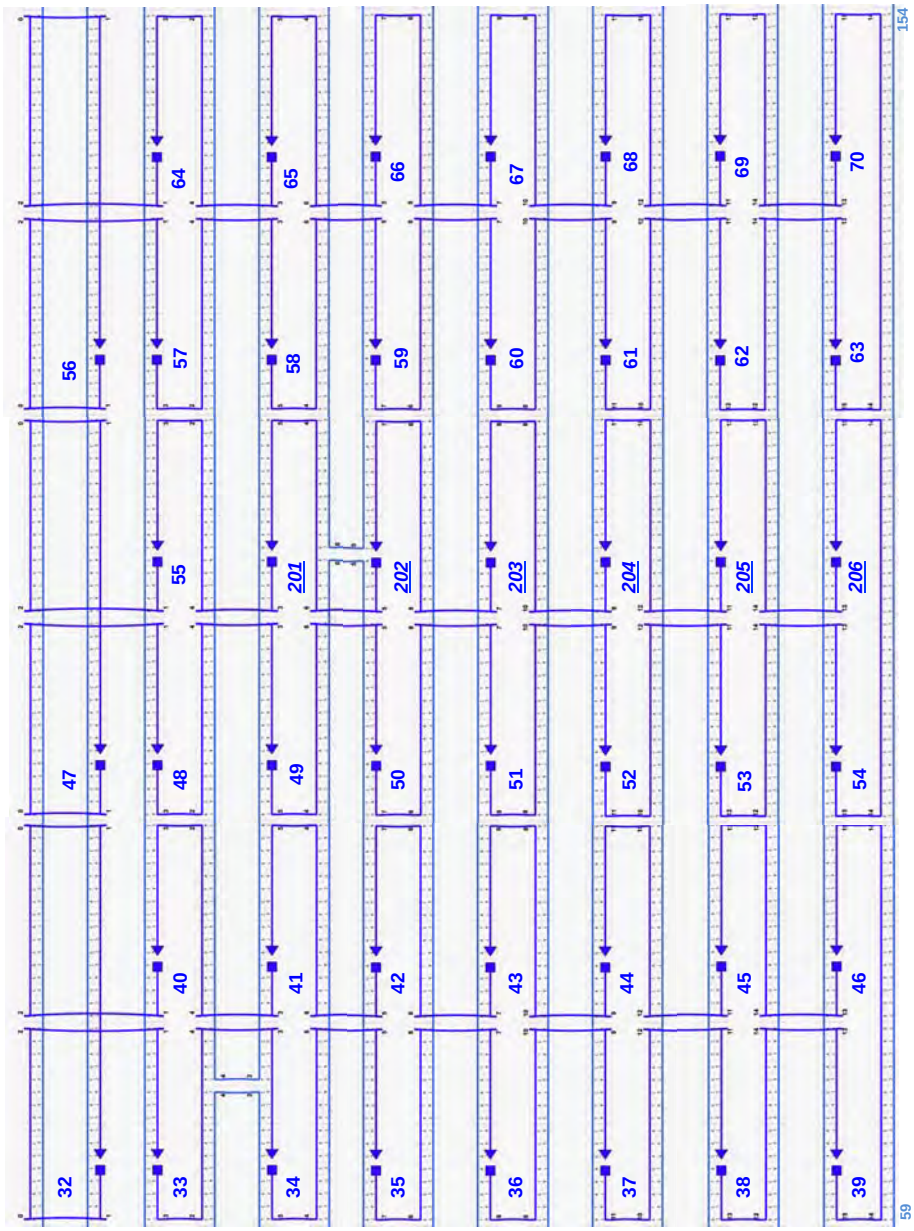

Origami Middle

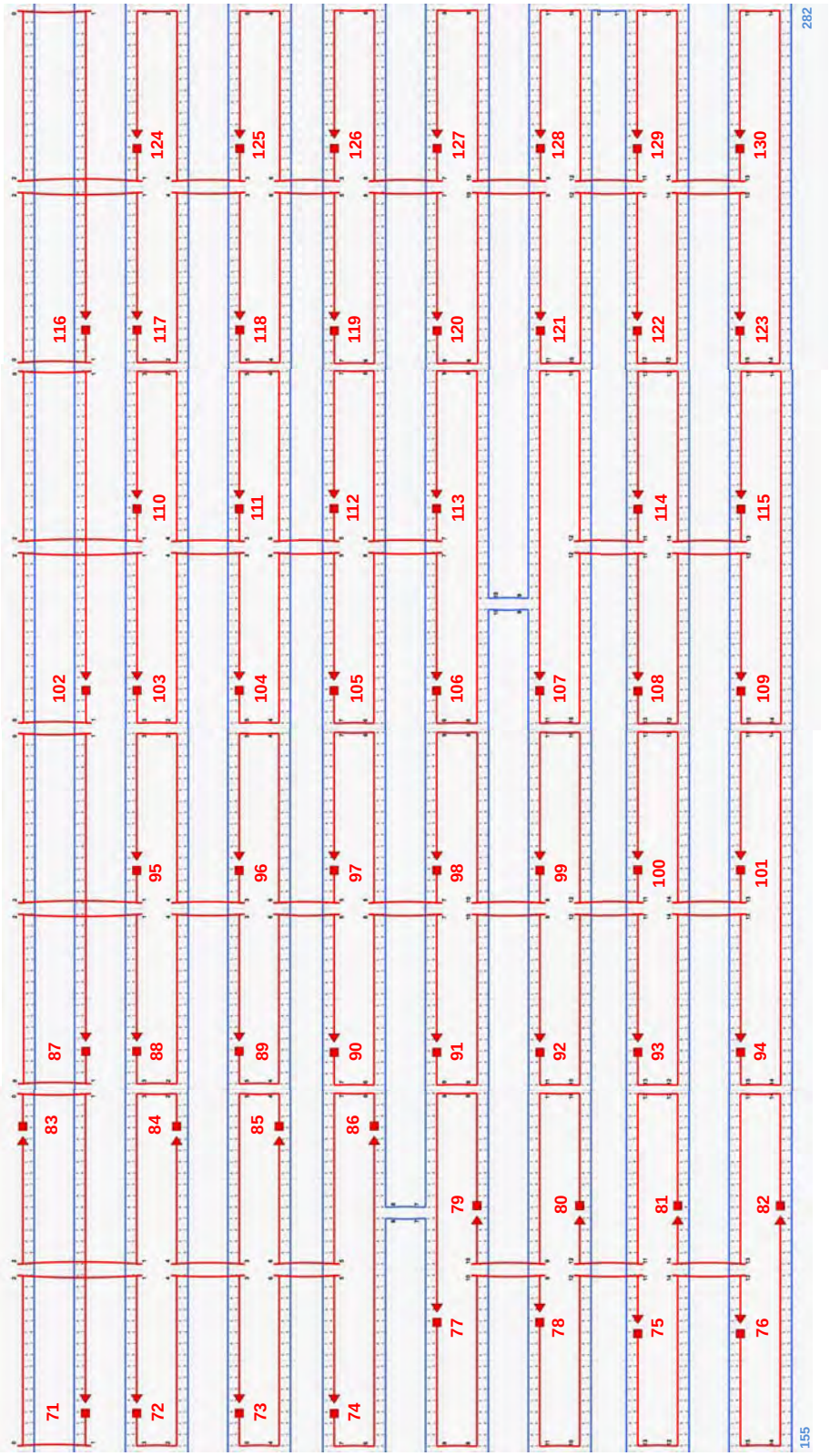

Capture Zone B

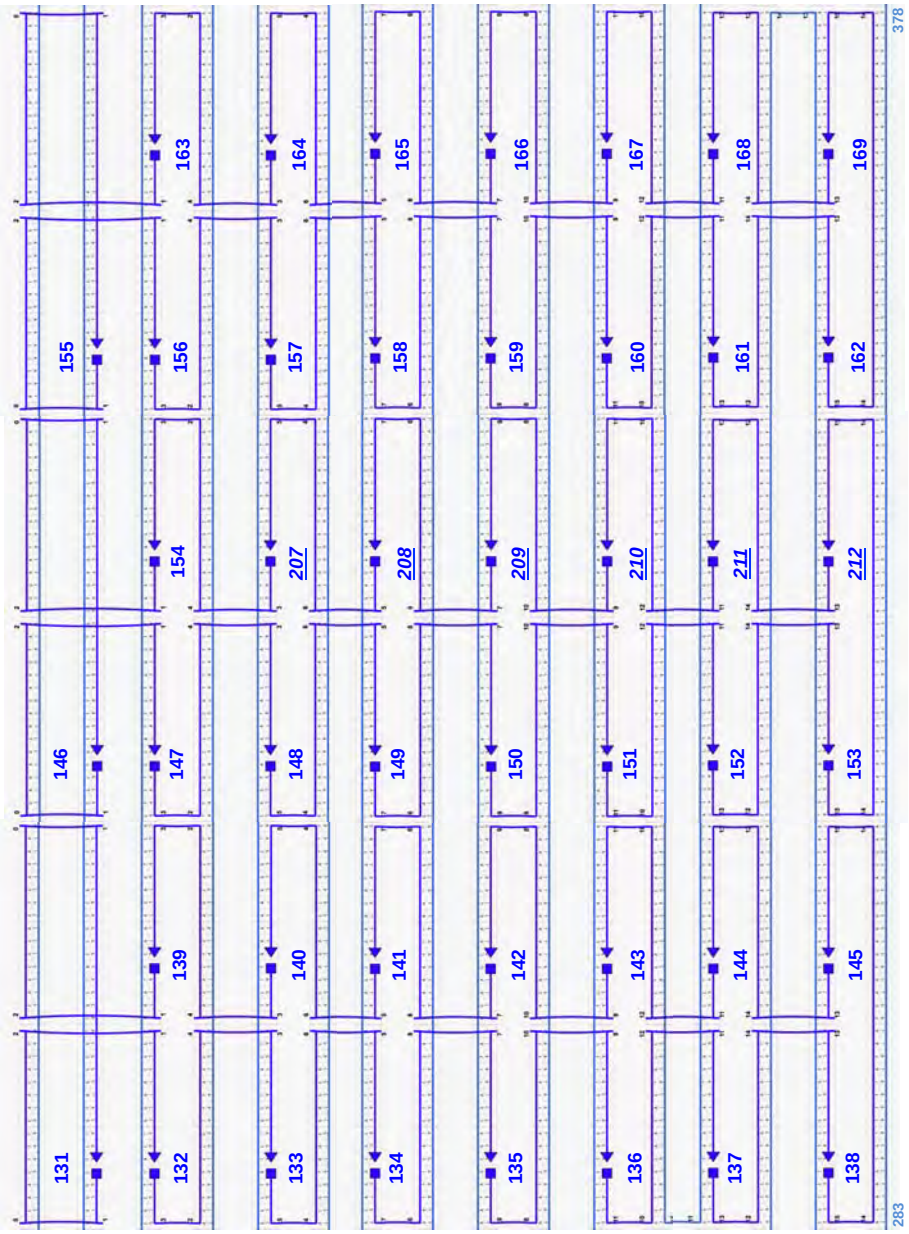

Origami Right

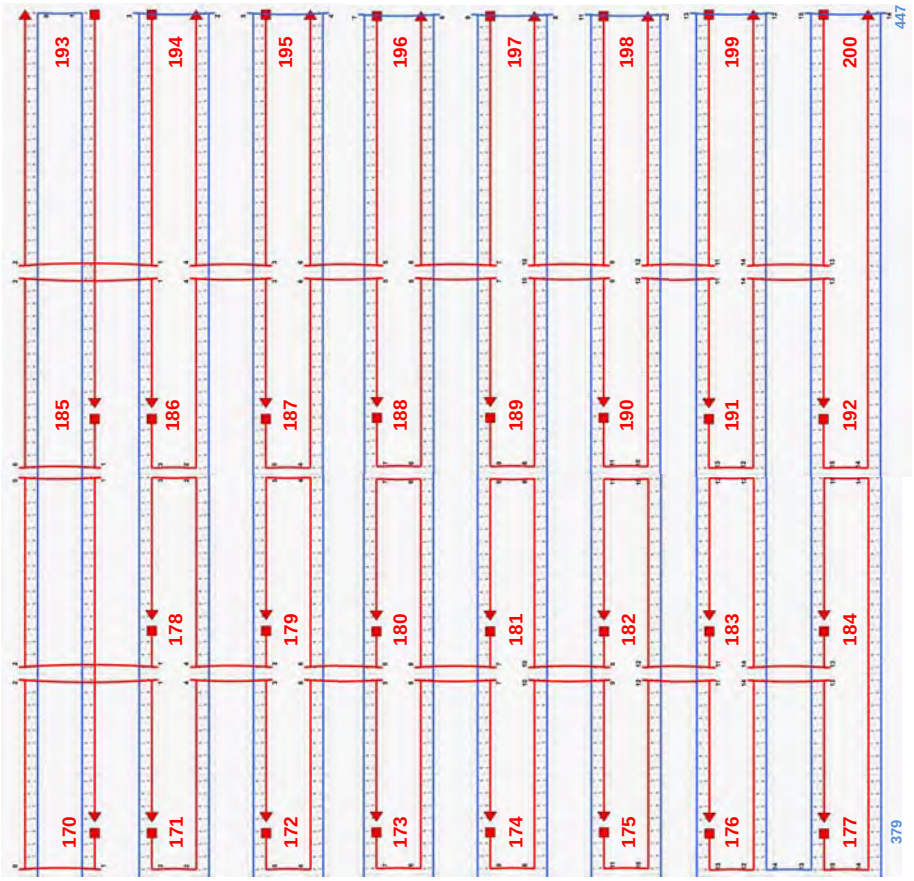

Appendix S2. DNA Origami Staple Strands

1	GACAGATGAACCTTCATCAAGA
2	GTAATCTTGACTCAACTTTAAT
3	CATTGTGAATTTAACCCTCGTT
4	TACCAGACGACCCTTTAATTGC
5	TCCTTTTGATAAATGCCTGAGT
6	AATGTGTAGGTATCGCACTCCA
7	GCCAGCTTTCCACCGTCTATCA
8	TAAAGGGAGCCCCCGATTTAGAGCTTGCGTCA
9	AAGGGCGAAAAGGCACCGCTTC
10	CAGGCGAACCGAACTGACCAACTTTGAAAGAG
11	ATTCAGCATAGGCTGGCTGACGGTGTACAGAC
12	TTTTATTGAGATGGTTTAATTAAGAACCGGAT
13	AAATAAAGAGCAACACTATCAACCTTATGCGA
14	TTGCGTCAGGATTAGAGAGTAGATAAAAACCA
15	AGGGTCATATATTTTAAATGCAGAGGTCATTT
16	TGGTGTATCGGCCTCAGGAAGAAAGATTCAAA
17	AAGGCGTACTCAGGAGGTTTGGAATAGGTGTA
18	TCACTTACCCAAATCAACGTGAGTAGTAAATT
19	GGGCAGAACTGGCTCATTATAATTACGAGGCA
20	TAGTGCGAGAGGCTTTTGCAAGCAAACTCCAA
21	CAGGGATGGCTTAGAGCTTAAAATTTTTAGAA
22	CCCTGAGAAAGGCCGGAGACGAGGGGACGACG
23	ACAGCCGGAAACCAGGCAAAAGAACGTGGACT
24	CCAAACGGGGAAAGCCGGCGAACGTGGCGAGAAAGGAAGAGTCCACTA
25	GCCCAGTACCGCCACCCTCACCGGAACGAGGCGCAGACGGTCAATCAT
26	GAACAACAAAGCTGCTCATTGATATAAGTATA
27	AAGGACCAGTCAGGACGTTGCGAGAAACACCA
28	CGGAAAAGAAGTTTTGCCAGACATAACGCCAA
29	ATAAATTGCTGAATATAATGAGCGAACCAGAC
30	GTTTAGTCAAATCACCATCATTCAACGCAAGG
31	TTAAGCGCCATTCGCCATTCGTGCATCTGCCA
32	CTTAGGAACCGCCACCCTCAGTGCCGTCGAGA
33	GGGTTCAGTGAATAAGAAGACCGCCAGCTTGC
34	CCTGAGGAAGAAAAATCTACGTTCAACTAATG
35	CAGATAGGGGGTAATAGTAAATTAATTCGAGC
36	TTCAACTGTAGCTCAACATGTCGGGAGAAGCC
37	TTTATATATGATATTCAACCGTGGGCGCATCG
38	TAACCAGGCTGCGCAACTGTTTGTTCCAGTTT
39	GGAACAAGGGAAGAAAGCGAAAGGAGCGGGCGCTAGGAGATAGGGTTG
40	ATAAGAACCGCCACCCTCAGATCGAAATCCGCGACCTGCTCCATGTTA
41	ACCAGAAAAGGGCGACATTCAGTACCAGGCGG

42 CCACATTAATAAAACGAACTATCATATGGTTT
43 GCGTTATGTTTAGACTGGATAATTTAGGAATA
44 TTTTGTTTAAATATGCAACTACTTCAAATATC
45 GTAGATTCTAGCTGATAAATTCCCTGTAATAC
46 AGTGTGGGAAGGGCGATCGGTGTCACGTTGGT
47 TTGTGGCCACCACCCTCATTTAGCGGGGTTTT
48 GCTCAACCGATTGAGGGAGGGACAATCAATAG
49 AAAATACGGAACAACATTATTAGATTCATCAG
50 TTGAGGCGTCCAATACTGCGGGAGGAAGCCCG
51 AAAGAAAGTACGGTGTCTGGAACCAAAAACAT
52 TATGAAATGCCGGAGAGGGTAGACCGTAATGG
53 GATAGGCGGGCCTCTTCGCTATCAAAAGAATA
54 GCCCGGCGCTGGCAAGTGTAGCGGTCACGCTGCGCGTCAAAATCCCTT
55 GGATTTCAGGGATAGCAAGCCCGGAGATTTGTATCATCGCCTGATAAA
56 TACAACAATAGGAACCCATGTGGCTGAGACTC
57 CTCAAGAAATTATTCATTAAAGCAAAGACACC
58 ACGGAGCGCCCAATAGCAAGCAGCAAGCCGTT
59 TTTATCATTGAATCCCCCTCAAGAAGCAAAGC
60 GGATTACAGTTGATTCCCAATAAAGCCTCAGA
61 GCATACTACAAAGGCTATCAGGTCGGATTCTC
62 CGTGGAAGGGGGATGTGCTGCGTGGTTCCGAA
63 ATCGGAACCACCACACCCGCCGCGCTTAATGCGCCGCAAAATCCTGTT
64 TAAGAACCGTAACACTGAGTTAGCGATTATACCAAGCGCGAAACAAAG
65 GAAACGGTGAATTATCACCGTCATGAAAGTAT
66 GAACAAAATCAGATATAGAAGAACATATAAAA
67 TAGTCAATGCTTTAAACAGTTGCACTCATCGA
68 GCAATTCTGCGAACGAGTAGACCTGACTATTA
69 AACCCGTCATTGCCTGAGAGTAGCAAAATTAA
70 TGATGAAGGCGATTAAGTTGGGAGCGAGTAAC
71 CCCCTCGTCACCAGTACAAAACCTATTATTCT
72 GAAACACCGACTTGAGCCATCATACATAAAGG
73 TGGCGCTTATCCGGTATTCTTATTAAACCAAG
74 TACCCAGAAAACGAGAATGACCATATTTTAAC
75 ACATTAAATGTGTAACGCCAGGGTTTTTTTGC
76 CCCAGCAGGCGTACAGGGCGCGTACTATGGTT
77 TCAGGTCTTTACTTTAGTTTGACCATTAGGCA
78 AGGCAAAGAATTCTGGAGCAAACAAGAGCATCA
79 ATTTCGCAAATAGAGACTACCTAATCAAAAA
80 ATGAACGGTAATCCAATAAATCATACAGATAC
81 TCACGACGTTGTCCTGTAGCCAGCTTTAATCG
82 GCTTTGACGAGAAGCGGTCCACGCTGGCCCAG
83 TAGCAGAATACACTAAAACACTCATCTTTGAC
84 GCCACCCTGCCTATTTCGGACTACAACGCCTG

85 CGTTGCAAACGTAGAAAATATTGGGAATTAGA
86 CTCCTCATTCCAAGAACGGGAAGAACGCGAGG
87 CAAAATTCCACAGACAGCCCATAAACAGTTAA
88 TGCCGCAAAATCACCAGTAGATTACGCAGTAT
89 GTTATTAGCGAACCTCCCGACGGCTGTCTTTC
90 CTTAGGCTTAGGTTGGGTTACAAAATCATAGG
91 TCTGGGTCAATAACCTGTTTAGTAGTAGCATT
92 AACATCGTAAAACTAGCATGAATTCGCGTCTG
93 GCCTTAAAACGACGGCCAGTCTGAGAGAGTTG
94 CAGCCACGTATAACGTGCTTTCCTCGTTAGAATCAGCCTTCACCGCCT
95 CCGTTCATAGTTAGCGTAACCGAAGGCACCAACCTAAAACGAAAGAGG
96 CCTTCACCATTACCATTAGCGAGTAACAGTGC
97 TAATCTTGCGGGAGGTTTTGATGATTAAGACT
98 TTATTATAACTATATGTAAAGAAACCAATCAA
99 TAATAGCTATATTTTCATTTTCAATAGTGAAT
100 AAATTCAATCATATGTACCCCATCAATTCTAC
101 GGCCGCCAAGCTTGCATGCCGAACGCCATCAA
102 ACTAGATCTAAAGTTTTGTCACGGGGTCAGTG
103 CCTTAAGGCCGGAAACGTCAACCCAAAAGAAC
104 TGGCAAGCCTTAAATCAAGAAATTTACGAGCA
105 TGTATGCTGATGCAAATCCAAAGACGCTGAGA
106 AGAGGGGGCGCGAGCAATCCTGATTGTTTGGATTATAGCGATAGCTTA
107 GTGGCGGTTGATAATCAGAAATTTTTTAACCA
108 ATAGTGCAGGTCGACTCTAGGGCAACAGCTGA
109 TTGCAGCGGGAGCTAAACAGGAGGCCGATTAAAGGGTTTCACCAGTGA
110 TTTAGTCTTTCCAGACGTTACCATTAAACGGGTAAAATACGTAATGCC
111 GAATCCAATGAAACCATCGACTGGTAATAAGT
112 TCCTTTAGTTGCTATTTTGCGCAATAATAACG
113 GATTATCGCAAGACAAAGAAAATAATATCCCA
114 GCTCAAGCCCCAAAAACAGGATGATGGCAATTCATCAATATTGAAAAG
115 GACGAGGATCCCCGGGTACCTTTGTTAAATCA
116 GTTTGTAAATGAATTTTCTGATGATACAGGAG
117 TGTATAGCAGCACCGTAATCAGGAAACCGAGG
118 AAACACCCAGCTACAATTTTAGTCCTGAACAA
119 GAAACGCGAGAAAACTTTTTGAATCCTTGAAA
120 ACATACTTCTGAATAATGGATATTCCTGATTA
121 TCAGAAGATTGTATAAGCAAAAATTCGCATTA
122 AATTGAGCTCGAATTCGTAACCAGGGTGGTTT
123 TTCTATTTTAGACAGGAACGGTACGCCAGAATCCTGGTTTGCGTATTG
124 TTTGTATGGGATTTTGCTAATGAGGACTAAAGACTTTTTCATGAGGAA
125 CAGAAGTAGCGACAGAATCATCATACATGGCT
126 GATAATCCTGAATCTTACCAGAACAAAGTTAC
127 CTTACAAATATATTTTAGTTTTATCAACAATA

128 ATCAAGGGTTAGAACCTACCAATTAATTTTCC
129 GTTAATATTTAAATTGTAAAAGCGGAATTATC
130 GGCGTCATGGTCATAGCTGTCGTTAATATTTT
131 GGCTTACAACTTTCAACAGTTACCGTTCCAGT
132 AAGCGAGTTTGCCTTTAGCGTAAGTAAGCAGA
133 TAGCCACGCTAACGAGCGTCTTGCAGAACGCG
134 CCTGTAATTTCATCTTCTGACGTAAATCGTCG
135 CTATTATATCAAAATTATTTGAGAAACCACCA
136 GAAGGGCCTGCAACAGTGCCAGGTCAGTATTA
137 ACACCTTCCTGTGTGAAATTGCGCGCGGGGAG
138 AGGCGAGAAGTGTTTTTATAATCAGTGAGGCCACCGATTAATGAATCG
139 AATTTTCAGCGGAGTGAGAATCGGAACGAGGGTAGCAACGGCTACAGA
140 AAGAACAGACTGTAGCGCGTTCGCAGTCTCTG
141 GCTAATTCCAGAGCCTAATTTAAGCCCTTTTT
142 CTTCTCTAAATTTAATGGTTTCAACATGTTCA
143 AACAACACGTAAAACAGAAATGAATAACCTTG
144 GAGGCCGCTGAGAGCCAGCAGTCATTTTGCGG
145 GCCAATTATCCGCTCACAATTAAAACAGAGGT
146 AGCATAGAAAGGAACAACTAAAAGCCAGAATG
147 GAAAGTTCATCGGCATTTTCGAATAGCTATCT
148 TACCGGCCAGTTACAAAATAAAGACGACGACA
149 ATAAAGAAATACCGACCGTGTATCAATATATG
150 TGAGTAAAGAAATTGCGTAGAAGTTTGAGTAA
151 CATTACAAATGAAAAATCTAAACCACCAGCAG
152 AAGATCCACACAACATACGAGTGTCGTGCCAG
153 CTGCAGTAAAAGAGTCTGTCCATCACGCAAATTAACCTTCCAGTCGGG
154 CATTAAGGAATTGCGAATAATGGATCGTCACCCTCAGCAGCGAAAGAC
155 TTGCGAATTTTTTCACGTTGACTTGATATTCA
156 CAAACTAGCGTTTGCCATCTTCCAATAATAAG
157 AGCAATCCCAATCCAAATAAGAAGTACCGACA
158 AAAGGAATAAGAATAAACACCGAATTACCTTT
159 TTTAACAGATGAATATACAGTAAATCCTTTGC
160 CCGAAACCTCAAATATCAAACCCTAAAACATC
161 GCCATTAAAGCCTGGGGTGCCGCGCTCACTGC
162 CCGCTGTTGTAGCAATACTTCTTTGATTAGTAATAACTCACATTAATT
163 TTGGCAAATCTCCAAAAAAAAAGGCTTGCAGGGAGTTAAAGGCCGCTT
164 TAAGCTTCATAATCAAAATCAAGGTCAGACGA
165 ATATAAAACGATTTTTTGTTTAAGAATTGAGT
166 CATTTGGAATCATAATTACTAGTAATAAGAGA
167 GTATTAACAGTACCTTTTACATTTAACAATTT
168 ATAGCCCTCAATCAATATCTGTTCGACAACTC
169 GCGTTTAATGAGTGAGCTAACTGCGCGAACTG
170 GCTGGGCTCCAAAAGGAGCCGACAGGAGGTTG

171 AGGCCCGGAACCAGAGCCACCAGAGAGATAAC
172 CCACAACGTCAAAAATGAAAAGGCATTTTCGA
173 GCCAGAAAAAGCCTGTTTAGAACAAAATTAAT
174 TACATCGGGAGAAACAATAATAGACTTTACAA
175 ACAAGTCAGTTGGCAAATCAGGCTATTAGTCT
176 TTAAATTTACATTGGCAGATTCGTCTGAAATG
177 GATTATCACTTGCCTGAGTAGAAGAACTCAAACTATACATTTTGACGC
178 CATTTTTAATTGTATCGGTTCGCCCACGCATAACCGATATATTCGGTC
179 ATATCACCGGAACCGCCTCCAGCCGCCGCCAG
180 GCAGATAGCAGCCTTTACAGAATTGAGCGCTA
181 AGAATATCATATGCGTTATACATGTAATTTAG
182 GTATCGGATTCGCCTGATTGAAACAAACATCA
183 GAATACAGTTGAAAGGAATTGAGGATTTAGAA
184 TCAATCACCAGTCACACGACGACAATATTTTT
185 ACCATTATCAGCTTGCTTTCGCCAGAACCACC
186 ACCAGCTCAGAGCCGCCACCCAACAAAGTCAG
187 AGGGTAGAGAATAACATAAAATATTTAACAAC
188 GCCAACAAATTCTTACCAGTAGCAAAAGAAGA
189 TGATGCTTTGAATACCAAGTTAATAGATAATA
190 CATTTGAGGAAGGTTATCTAAAAGAATACGTG
191 GCACACAGTAATAAAAGGGACGCTCATGGAAA
192 TACCTCGGCCTTGCTGGTAATATCCAGAACAATATTACCGCC
193 TGATACCGATAGTTGCGCCGACAATGACAACA
194 CCACCACCCTCAGAGCCGCCAAGGTGAATTTCTTAAACAGCT
195 GAGAATTAACTGAACACCCTGTCAGAACCGCCACCCTCAGAG
196 GGGCTTAATTGAGAATCGCCAACAGGGAAGCGCATTAGACGG
197 TTATTCATTTCAATTACCTGATAAAGCCAACGCTCAACAGTA
198 AACTAATAGATTAGAGCCGTCACAAAATCGCGCAGAGGCGAA
199 ACCCTTCTGACCTGAAAGCGTAATATCTTTAGGAGCACTAAC
200 AGCCATTGCAACAGGAAAAACATTCTGGCCAACAGAGATAGA

DNA Origami Capture Strands

201 TTGTCAAGGTAAATATTGACGGAGAAGGATTA TTTTT TGATATAGGTGAGTA
202 TAGAAACAGGGAATCATTACCATAAGTTTATT TTTTT TGATATAGGTGAGTA
203 ATTAAAATCGTCATAAATATTTTTCATCGTAG TTTTT TGATATAGGTGAGTA
204 GTTGTAGTTTCATTCCATATAGCATCAAAAAG TTTTT TGATATAGGTGAGTA
205 GGATTGCTATTTTTGAGAGATAAGCTAAATCG TTTTT TGATATAGGTGAGTA
206 ATAAATTACGCCAGCTGGCGAGAACAAACGGC TTTTT TGATATAGGTGAGTA

207 ATAGCGTCATAGCCCCCTTATAAATAAATCCT TTTTT TGATATAGGTGAGTA
208 TGTCCACAGCCATATTATTTAGAAACAATGAA TTTTT TGATATAGGTGAGTA

209 CATAAGATAAATAAGGCGTTATAAAGTAATTC TTTTT TGATATAGGTGAGTA
210 TTAAATTTTCAGGTTTAACGTTGGAAACAGTA TTTTT TGATATAGGTGAGTA
211 AACGAAGCATCACCTTGCTGACGTTATTAATT TTTTT TGATATAGGTGAGTA
212 AAACCCCGGAAGCATAAAGTGTAAAAATACCG TTTTT TGATATAGGTGAGTA

APPENDIX 2: Second Generation Origami Design and Components.

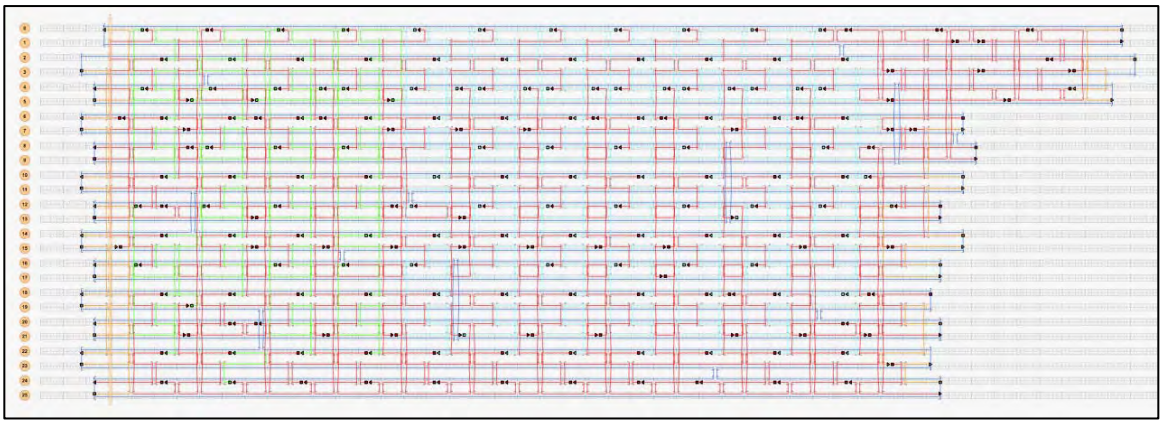

1. GAGCACCGGAACCGCCTCTCAGAGAGGT
2. TCAGCCCATGTACCGTAAACCACCCCCTCAGATTGT
3. TTTTAGATAAGTCCTGAATGTTCAGTTAGCCGTGAT
4. GAACAGGTCGGTAGTAGGTTAACCTGTT
5. AATATTTCAACGCAAGACATTATACTAATAACTC
6. TGATAGATAATACATTCTTTAGGGTTTCCTTAAA
7. ACTAAATCACCGGAACCAGCCGCCAGATA
8. TAAGTATAGCCCGCCTTTACAGAGGAAA
9. CACTAATAATATCCCATCAGACGACCGGTCAAAGTT
10. ATACGAGAAAACTTTTTCCTTTTTCTATTAAATAA
11. CCATTTTTAGAACCCTGCTAAATATCCAATAGCT
12. AGACAGTCGGGAAACCTCATCCACACAA
13. ACGTTCCACATTGCCATCTTTTCAAGAGCCGATAA
14. TCAACAACGCCTGTAGCAATTTTTTACAGGGACCCA
15. AACACGAGCATGTAGAAAAAGGTAAACTGACAACT
16. AATATTTTAGTTAATTTAATCATAGAATCCTTAAA
17. TGATTTAAATGCAATGCAATAAAGAGGCAAAGTAA
18. AGAAACAATTCGACAACAATCAACGTCACACATTA
19. GCGTTCATAGCCCCCTTAAGGAGGTGTTT
20. CGTGACAGCCCTCATAGTCCCAATGAGAATTCTAA
21. ATAAATAATCGGCTGTCAGAGAATGACAGATCTCA
22. AGTTGACCTAAATTTAAAGTCAATTAGCTTATTTT
23. TTAATGGAAACACCAGAAGGAGCGGGTT
24. AAAAAATCCTTTGCCCGTCAATATGGGACATACGC
25. CAATTGTCGTCGTTTTCATCGGCACGATTGGAGAA
26. TCGGAACGATCTAAAGTTAATAAACAACAAAGCGAA
27. ATAATCATTCCAAGAACGGCATTTCCAGGCGTTGC
28. TGAATATAATACAATAGTAAAATGAACA
29. TGCAGGGTGAGAAAGGCGTAACATTTCCTGAGATT
30. ATTTTAATTTTAAAAGTCCTCAAAATAGAACCATG
31. CAGGTAAATGCTTTAGCGTCAGACAACAAATAAGA
32. GCGCTTTCCAGACGTTAAGCCTAAAGCGCTATACG

33. CCAAAACCAAGTACCGCCCAACATCCTTCATTGCG
34. TTTTAAGGCGTTAAATAGGCTTTTCGTCCAAAAAA
35. AAGAGTCAAATCACCATTTAAATCCAATTCAAAGG
36. CCAATAGGAACGCCATCCTAAAGCAGCGTAACATT
37. CAAGATTTTGTAGCGACAGAATCAGCCAGAAATTC
38. TTGCAATTTTCTGTATGGCGCTAACACCCACAGGGT
39. GTCGAGAACAAGCAAGCGAATCGCACAAGAACTTT
40. TTTACACCGGAATCATAATAAAAACATAAATGATG
41. AATATATTCAACCGTTCAAAATTCATTGTTTCGCT
42. TAAATTCGCGTCTGGCCAGCCAGCGACAATACAGA
43. ACAAACAGTTTCGATAGCAGCACCGTCTGAATCTGC
44. CAGCTAAACAACTTTCATTTTATCCCCAATAATGA
45. ATCATTTTCATCGTAGGTCAACAGCCCAAATAGAG
46. GCTGAAAAAGCCTGTTTACCCTCGCCTCAAATCAA
47. CCATAAATTAATGCCGGTGTAAACAATAATGGGCG
48. ATAAGCCAGCTTTCATCCTGCAACTTAGTCTATCG
49. TTGTAGAAAGAAACGTCACCAATGAGCGTCACGTA
50. CATCAGCGGAGTGAGAACTATTTTCAATGAATTGA
51. CCAACCGCGCCCAATAGTTACCAGTGCTCATAAAC
52. AAGTATGCGTTATACAAAGTAAGACAGAAAACGCA
53. CACAGCTATTTTTGAGATGTATAATACCATAGGCT
54. ATAAATGTGAGCGAGTAGGCGGTCGATAGCCCTGA
55. GAAATTGCGACATTACCATTAGCATGATACAAGTG
56. CGGGAACAACTAAAGGAGCCTTAACTTACCGGTAG
57. AGAATCAGATATAGAAGATACCAGTTGCCCTAAAG
58. AGAAAAATCTACGTTAACCAAAAGAATCAAAGAAT
59. TACAAAGGCTATCAGGTAAGCCCCACGTAAACAAA
60. ACAGTCGGATTCTCCGTCAGAAGATTAAAAAATTA
61. ATATAGTAAAAGCAGCGAGCAGATCACGGAATAAG
62. CACATAATAATTTTTTCCGACTTGAAAAGTAAAAG
63. AGGCGGTATTCTAAGAAGATTTTAGAACGAGTCGC
64. ACTGAACTAACGGAACAAAACTAATCCTGACTACGG
65. ATATGAGAGTCTGGAGCTACCCCGATTGCGTCTTC
66. TGGTGCCGGACGGGGACGACGACACGTT
67. TTTATCAACAATCAGGGATAGCAA
68. GCTGATGCAAATAGAACGCGCCTG
69. GTGTAAAGCCAATTGCGGGCGAAAAACCGTCTATCA
70. GCATTTCATTTATTAGATGCGAACGCTGCTCCGAT
71. TCCCAATTCTACATTTCTATAT
72. TAGCTATATTCAATTCTGACCC
73. AAATCTCAGAAACTCAGGTCAGAACCGCCACCCCC
74. GTATCACCGTCCGCCACTCA
75. ATCATCGCCTATGTTACCTAATGCCCAATCGCAAGACAGTTG
76. TAGAGGATCCCATAGCTAGCACTAGTGAACCATCACCCGTCA
77. GGTGCAAATGGTCAAAATAACAGTGAA
78. CATACGAGCCCGCTTTCACGTGGACTCCAACAAATCAAAAAATATTGA
79. AACACAAGAAACAGAGCCCACT
80. AAGTTGCGCTCACTGCCGGAAGCAGTGT
81. GGATACCAAAAGATAAAAGGCTTAGAAGAACGAAC
82. TCATTCCATAATCGTCGAACCT
83. CGAGCGGAGATACCGCCACCGGAATCCACCACCCTCAGAGAGC
84. CAAAGTACAAGCGCAGAGACA
85. CACTTTCGTCACCAGTAATGAAAATAG
86. CCTTGCTTCTCATTAACCGGTTGTTTAGAAGTATTAGAGAGG
87. TGCATGCCTGATTGTTAGTTATCTGTTTTTTGGGGTCGTTAA
88. ATATTCTGTCCCTAATTTGTCAAAACAA

89. AATTCTTTACAGCATAAACATATATGAGACTACAA
90. AAGTCCGCTCACAATGAAGTGCCAAAA
91. TCATTGAGTGATTAATTTGTCTGGATCATAAGCAA
92. TTTACATTGGGTCGTGCACAAGAGTCCACTAAGGTGCCAGG
93. GTGCCGTCGACATAAAAGTTT
94. GCGATTATACGGAACCGAAGT
95. AAAGTACGGTTCCCTTAGGTC
96. TCAATATATGACAGGCACCTC
97. GCGCAGAATAAGAGGGTTCCAGAACCACCACCTAA
98. AACGACGGCCTTCACCAAGTTGAAGTAAAGCACTAAATGTT
99. ATTATTAAGCCTGAGTATTATCAACATCTTCACCGACAACCAATCAGAA
100. TAGCAGTACATGAAAACAATATGCCAACTTTTTTG
101. TGGACAGCTGCATTAATGGAAATGGGACCAGTCGACGTTGAAT
102. TCAATCGTCTAATCGGCTGAGTGTTGTTCCACGGAACCGTTGGCATCGT
103. ACCAGCGCATCAGGCGGCCGCCAGCATTGACTTAG
104. TGCTCAGTACTAGACGGCCAA
105. AACACTCATCGAAAGAGATAA
106. ACATGTTTTAATAGCGAAGTGAATATGTGTAGGTAAAGACAAAGAAACC
107. TTCCCAGTCAAATAAAACTGGTCACTAAAGGGAGCCCCATAG
108. GAAGTGGTTTGAGTAATATTTCCTTTTATTTATTA
109. TATAATTACCGATTAAGGCTGTAGGAA
110. GGTCAACGCGCGGGGAGCATTTTGTCTGGCCACGCCAGGAAT
111. GAAATACCTAAGGCGGTAAGAATAGCCCGAGCGATTTACCCTCAAAACG
112. TTATTGCGGAATTCAAATGA
113. GGATTAGGATCACCCTGAGCC
114. AGAGGCAAAAGTACAGATCGAGCCAAATACCGACCGTGGCCAGAGGGGG
115. ATTTCATTTGCATCATATATC
116. CGGTGAATACAAACTGAATAGCGGGTGAGGCAGGTCAGATTT
117. AAGTTGGGTAAACAGAGTATCAAAGAGCTTGACGGGGAAAAT
118. CAGTACATTTTTTAGACAGCTTAACAT
119. AAAAGGCAGAGGGTATTGTTA
120. CAAAATTAATATGATGGAGCTCATTTTTTGACGGAGACAAGTTTTTGAT
121. CAATTGCGTATTGGGCGAAACGCTCCTTCTGGCAAGGCTTAT
122. GCAACAGGAACCAGGGTGCAAAATCCCTTATAAGCCGGTGCTGAATTAA
123. AGGCCCTAAAATCAGAGGCCTCAAGCCTTGATATTCACATGTA
124. GGCTGAGACTGTAATTGTTTG
125. AAGGCACCAATGGCTGAGTAA
126. GATGGCTTAGTGGATAGGCAA
127. GGGATGTGCTACCTGAAATCACCTCGAACGTGGCGAGAGAAA
128. TATCATCAAGTACTGCGTCATTTTCAA
129. ATAATTTTTGCAATATGAGCGAGAAGAATAAAACAACGACTCATCTTTC
130. TCGGGTTTTTCTTTTCACGCCAGCGAATACGCTGGCGATCAA
131. ACAATATTACCCAGTGATTGATGGTGGTTCCAAGGAAGGAAAAATAAAA
132. TGAAACATGAAGAGATAGAGC
133. AAAATACGTAAATCTTGCATA
134. TGATAAGAGGGAATCGTCCAA
135. ATGAAACAAAAATCCTGGCAT
136. GAGTATGCCACATATCAGAAGTATTAAATCCTCATTAAAAGT
137. ATTACGCCAGTGGCACAAGCAAATGGAAGAAAGCGAAAATCC
138. TGTTTTTGTTTAGCTGAGACGACGATTACTATAATTGACGTTTTTTTAC
139. TATAAAAGAAATTCATTATTGCTCCCGGATAATTA
140. TGTGACGGGCAACAGCTTAATATCTTTTTGAGCCTCTTGGAT
141. GCCTTGCTGGGATTGCCCCCAGCAGGCGAAAGGAGCGGCGCTGAGTTCC
142. AACAGAATTGACCTATTTGGAAAGCGCAGTCTAAT
143. CTATTTCGGAAGTTAAGCTGA
144. GGAAGTTTCCTTCATTATAGG

145.AGTACCTTTAGAATCCCTTTA
146.TTACCTGAGCACTTCTGGTTA
147.ATCGGTGCGGATGGCTAAGTGCCAGCGCTAGGGCGCTGGGTT
148.AAGCGGTCCACGCTGCAAGTGACACCGCAACATTATTTAAATAGA
149.GGTATTCATTTGCTTTACAGGATTCAACGTACTTT
150.TGCCTTCACCGCCTGGCTCAAACTTTAATGCTGGGAAGGAAG
151.GGGTTATCATAAGTATCACCAACGCAATCATTGCT
152.TTCATAAGAGATGCCCCTTACCGTTCCAGTAAAAC
153.TAAACAGTTACAAGAAAGCAC
154.GGACTAAAGAACAAAGCTATA
155.TCCAACAGGTAACAGTTGCAA
156.GAGGCGAATTTAGAACCGCAA
157.GCGCAACTGTGCGAACTAGTATTATAGCGGTCACGCTGTTGCAGC
158.CAACGGCTACATAAGGCTCAGGACGTTGGTCCAAGCAATTAG
159.TCATCAAAATAAAATCGCGAGAATCGGAAGCTCAG
160.CCCGGAAGATGATCTACGAGGCATATGA
161.GTAGAAGAACCCTGAGAGAGTTAGACAGGAACACTTGCCTAAAACCCAT
162.GTAATAACATCGGTACGCGATTAAAGGGATTCGCGTAAGAGGTGAACAA
163.TGAAGAGGCTATAGCAACAGTGCCTACATGGCTTTTGAAGGC
164.CCTTGAGTAATAGCTATATCA
165.CGAACCAGACGACCATAGAAT
166.ACCAAGTTACTATTTGCAAAA
167.GCGCCATTCGATCGCCATAAAACACCACCACACCCGCCAGGA
168.ACAATCAGAACATTGCCCATAACGTAAAACGGCTCATTGCTTATCTTTT
169.AAATTGCTTTAATCAGGGAGCTTCGACGAGAAACG
170.GGCCCAGAATCCTGAGATTCTTTGTACCGAAAACCAGGACAG
171.GTAGCAATACAGTGTTTAGCGGGAGCTAAACGCGCTTACCACCAGGGGA
172.AGGAAGCCCTCGGGGTCGGAGTGTACTGGTAGTAG
173.TAAGTTTTAATTTTAAGCGGG
174.GTTTTAATTCTCTTTACGCAG
175.ACAGCATCGGAACACCAAGA
176.ATTCGCCTGATAAAGAAGTTGATAAACGGCGGATTGACTGCC
177.CGAAGATAGCGAACCTCCACGTTGACAGCAAAATC
178.AGTTTGAGAAATGCGCCGCTACAGGAA
179.ACCGTGCTTTCCTCGTTAGGCGCGTGTGCATCCGT
180.ACCGAGATTTTAACAATAATTATAGTCAA
181.AATGTCATATGAAACAAGCACATTCCATTATTCTT
182.TCAGTTATAATCAGTGAGAATTAACGTATCGGGGC
183.CCATTTGGGAAAGAAAATAAACGCAAAGACACAGC
184.ACCAATTTATTTTGTCACAATCAATTTAGAGCAAA
185.TCTCCAAAAAACATAACCCAAAGTTGGATCGTCACCCTCTTG
186.AGTTGAGATTTACAAAGCGTTTACATCGGGAGACAG
187.GATGAAGCCCGAAAGACTTCAGAAGGGA
188.ATGCCGCGAGGCGTTTTATATTCGGTCATTGTTGA
189.GGAGTTACAACTTTAATCGCTGAGCCCACGAAGGCTCGAG
190.GGCTGAATTACACAGGTAGAAAGATTCATC
191.GTTTATGTCAAGGATAGGTCACGTTGGTGT
192.CTCCAGCCAGCTTTCCCCTCAGGCGTAACCACTATGGTTGCTTTGACGA
193.GCCGCTTTTGCGACCAGAAATAAAAGTCATATGGT
194.GCCAAAAGGTGGCAACATGGAAACCAACCATCGGCTTGCAG
195.GTAAATTATCACCGTCAAGC
196.TTACCCCGACTTCAAAAGGAGCCTTTTGACAACGAG
197.GTAGAAAATAATAACGGAGTTGCGCCGACAAAATT
198.GAAACGCAATACATACATAAGACAAAAGGGCGAAA
199.TGATGCTTTCGGAAATTATTCATTACATTCAAAAC
200.GGTGTCGGTTTATCAGCTTACCGATAATACCCAAA

201. AGAATGTTAGCACCGATTGAGGGAGGGAAG
202. ACCGCCACCTGTGTCGAA
203. ATCCGCGACAGTAGATTT
204. AGTTTGACCGGGGCGCGA
205. GCTGAAAAGCCGAGCTCG
206. AATTCGTAACCTAATGAG
207. GGGAGAAGCCTTCTATATGTAAAT
208. TTAGAGCCGTCATAATACTTTTGC
209. ATGGCCCACTACACAACTAATAGA
210. GCCCAATAGGAAAGCCGCCAC
211. TGAGCTAACTCACATTTGGGGTGTCATGGTCCGGGTAGTG
212. AGATGGGCGCATAAGATCGCTGTCCATCACGCAGCC
213. GCACGTATAACGAGTAAAAGA
214. ATACAGAATCGATGAACGGTAAT
215. AAGATTAAGAGGGTTTAATTTAAG
216. GTAACAGTACCTGATTGCATCAAA
217. CGTAAAACTAGCAACGTCAGATGAATATACA
218. TCCTTATTACGCAGTACTGGCATCTTAAACAGCT
219. GTAAATATTGACGAGGTGAAT

1.

1. Report Type

Final Report

Primary Contact E-mail

Contact email if there is a problem with the report.

mmmaye@syr.edu

Primary Contact Phone Number

Contact phone number if there is a problem with the report

315-443-146

Organization / Institution name

Syracuse University

Grant/Contract Title

The full title of the funded effort.

PECASE: New Synthetic and Assembly Methodology for Guiding Nanomaterial Assembly with High Fidelity into 1D Clusters and 3D Crystals Using Biomimetic Interactions

Grant/Contract Number

AFOSR assigned control number. It must begin with "FA9550" or "F49620" or "FA2386".

FA9550-10-1-0033

Principal Investigator Name

The full name of the principal investigator on the grant or contract.

Mathew M. Maye

Program Manager

The AFOSR Program Manager currently assigned to the award

Dr. Hugh DeLong

Reporting Period Start Date

01/01/2010

Reporting Period End Date

12/31/2014

Abstract

In year five of our grant we successfully completed a major grant milestone, and made progress and improvements in the areas where goals have previously been met. These accomplishments include: the first publication in the field on the self-assembly of quantum rods using DNA in which we used a patterned surface provided by DNA origami to control rod alignment and spacing (Section 1); published final results showing bioluminescence resonance energy transfer between firefly luciferase enzymes and rods that emit near infrared light (nIR), and improved long term stability and activity of the BRET nanoconjugates (Section 2). Finally, we completed a study that investigated ways to manipulate the 3D assembly of DNA-capped gold nanoparticles by using smart pH sensitive co-polymers, and transitioned that system to using elastin like polypeptides that have similar thermal- and pH responsive behavior (Section 3). We also successfully aquired and set-up an atomic force microscope purchased with AFOSR support. Two high impact articles were published, and one is in review. Four additional papers cite the grant, and three papers are in final stages of preparation.

Distribution Statement

This is block 12 on the SF298 form.

Distribution A - Approved for Public Release

Explanation for Distribution Statement

If this is not approved for public release, please provide a short explanation. E.g., contains proprietary information.

SF298 Form

Please attach your SF298 form. A blank SF298 can be found here. Please do not password protect or secure the PDF The maximum file size for an SF298 is 50MB.

AFD-070820-035_Maye.pdf

Upload the Report Document. File must be a PDF. Please do not password protect or secure the PDF . The maximum file size for the Report Document is 50MB.

MAYE_FA9550-10-1-0033.pdf

Upload a Report Document, if any. The maximum file size for the Report Document is 50MB.

Archival Publications (published) during reporting period:

(1) T.L. Doane, R. Alam, M.M. Maye* "Functionalization of Quantum Rods with Oligonucleotides for Programmable Assembly with DNA Origami" Nanoscale 2015, 7, 2883-2888.
(2) R. Alam, L.M. Karam, T.L. Doane, J. Zylstra, D.M. Fontaine, B.R. Branchini, M.M. Maye* "Near infrared bioluminescence resonance energy transfer from firefly luciferase-quantum dot bionanoconjugates" Nanotechnology 2014, 25, 495606.
(3) J. Gooch, A.A. Jalan, S. Jones, C.R. Hine, R. Alam, S. Garai, M.M. Maye*, A. Muller, J. Zubieta* "Keplerate cluster (Mo-132) mediated electrostatic assembly of nanoparticles" J. Colloid Interface Sci. 2014, 432, 144-150.
(4) C. M. Alexander, K. L. Hamner, M.M. Maye*, J.D. Dabrowiak* "Multifunctional DNA-Gold Nanoparticles for Targeted Doxorubicin Delivery" Bioconjugate Chem. 2014, 25, 1261-1271.
(5) S. Majumder, I.T. Bae, M.M. Maye* "Investigating the role of polytypism in the growth of multi-shell CdSe/CdZnS quantum dots" J. Mater. Chem. C 2014, 2, 4659-4666
(6) W. Wu, M.M. Maye* " Discrete Dipole Approximation Analysis of Plasmonic Core/Alloy Nanoparticles" ChemPhysChem 2014 (DOI: 10.1002/cphc.201402082).

Changes in research objectives (if any):

Change in AFOSR Program Manager, if any:

Extensions granted or milestones slipped, if any:

AFOSR LRIR Number

LRIR Title

Reporting Period

Laboratory Task Manager

Program Officer

Research Objectives

Technical Summary

Funding Summary by Cost Category (by FY, $K)

	Starting FY	FY+1	FY+2
Salary			
Equipment/Facilities			
Supplies			
Total			

Report Document

Report Document - Text Analysis

Report Document - Text Analysis

Appendix Documents

2. Thank You

E-mail user

Mar 28, 2015 10:57:53 Success: Email Sent to: mmmaye@syr.edu